

Asynchronous Load Balancing and Auto-scaling: Mean-Field Limit and Optimal Design

J. Anselmi

Univ. Grenoble Alpes, CNRS, Inria, Grenoble INP, LIG, 38000 Grenoble, France.
jonatha.anselmi@inria.fr

April 6, 2022

Abstract

We introduce a Markovian framework for load balancing where classical algorithms such as Power-of- d are combined with asynchronous auto-scaling features. These allow the net service capacity to scale up or down in response to the current load within the same timescale of job dynamics. This is inspired by serverless frameworks such as Knative, used among others by Google Cloud Run, where servers are software functions that can be flexibly instantiated in milliseconds according to user-defined scaling rules. In this context, load balancing and auto-scaling are employed together to optimize both user-perceived delay performance and energy consumption. In the literature, these mechanisms are synchronous or rely on a central queue. The architectural novelty of our work is to consider an *asynchronous* and *decentralized* system, as in Knative, which takes scalability to the next level.

Under a general assumption on the auto-scaling process, we prove a mean-field limit theorem that provides an accurate and tractable approximation for the system dynamics when the mean demand and nominal service capacity grow large in proportion. We characterize the fixed points of the mean-field limit model and provide a simple condition telling whether or not all the available servers need to be turned on to handle the incoming demand. Then, we investigate how to design optimal auto-scaling rules and find a general condition able to drive the mean-field dynamics to delay and relative energy optimality, a situation where the user-perceived delay and the relative energy wastage induced by idle servers vanish. The proposed optimality condition suggests to scale up capacity if and only if the mean demand exceeds the overall rate at which servers become idle-on, i.e., idle and active. This yields the definition of tractable optimization frameworks to trade off between energy and performance, which we show as an application of our work.

1 Introduction

Load balancing is the process of distributing work units (jobs) across a set of distributed computational resources (servers). Exogenous jobs join the system over time through one or more dispatchers, and these route each of them to one out of N parallel servers for processing. Then, each job leaves the system upon service completion at its designated server. In large architectures, each server has its own queue, as this enhances scalability, and jobs are immediately dispatched upon their arrival. Given the stringent latency requirements of modern applications, breaches of which can severely impact revenue, load balancing techniques are usually designed to optimize delay performance, and popular examples are Power-of- d [24] and Join-the-Idle-Queue (JIQ) [21]. Closely related to load balancing, *auto-scaling* is a term often used in cloud computing to refer to the process of adjusting the available service capacity automatically in response to the current load [29]. In this context, auto-scaling techniques are meant to control capacity (N) over time to avoid performance degradation, which yields unacceptably large delays, and overprovisioning of resources, which yields high infrastructure and energy costs. Google Cloud Run, Amazon Elastic Compute Cloud (EC2), Microsoft Windows Azure and Oracle Cloud Platform are examples of platforms that offer auto-scaling and load balancing features. Users of these platforms deploy their applications defining how the system should scale up resources in front of an increased load. Modern auto-scaling mechanisms are extremely reactive in the sense that they adapt capacity relying on fresh observations of the system state

rather than historical data. This especially holds true in *serverless computing platforms*, or Function-as-a-Service, which nowadays provide the convenient solution to deploy any type of application or backend service [22].

Most of existing performance models for load balancing assume that the available service capacity, N , remains constant over time even when designed for cloud computing systems [37], i.e., auto-scaling is not taken into account. Nonetheless, auto-scaling mechanisms are frequently employed in cloud applications and affect delay performance. This does not mean that classic load balancing models are inadequate for cloud systems but that they assume that auto-scaling operates at a much slower timescale than load balancing. Essentially, this means that jobs do not see any change in the overall available capacity because they move much faster than servers. This makes sense if servers are interpreted as physical or even virtual machines because setup times are of the order of minutes if not longer [15] while in typical applications hosted in cloud networks job service times are about ten milliseconds. The large body of literature on load balancing, reviewed in Section 5, is undoubtedly the proof that this timescale separation assumption is well accepted by researchers and practitioners. In the context of serverless computing however, a server is interpreted as a software function that can be flexibly instantiated in milliseconds [40, 41], i.e., within a time window that is comparable with the magnitude of job inter-arrival and service times, and with negligible switching costs. Here, auto-scaling mechanisms are extremely reactive and the decisions of turning servers on or off are based on instantaneous observations of the current system state rather than on the long-run equilibrium behavior or historical data. Therefore, the timescale separation assumption above becomes arguable [22] because it would mean to assume that job dynamics achieve stochastic equilibrium between consecutive changes of N , i.e., in milliseconds.

While there is a large body of literature investigating load balancing and auto-scaling *separately*, very little has been done when both are applied jointly within the same timescale. Most of existing works focused on synchronous and centralized architectures where all servers share a common queue [15, 22], where synchronous means that scale-up and dispatching decisions are taken simultaneously. In typical cloud architectures however, no central queue is maintained as it would affect scalability. A notable exception is [26], where the authors consider a synchronous but decentralized architecture where each server has its own queue; see also [16]. In particular, they synchronize JIQ [21] with a specific auto-scaling strategy and analyze the resulting performance in the mean-field limit; see Section 5 for further details. Also our framework considers a decentralized architecture but the key novelty is that load balancing and auto-scaling operate *asynchronously*; the term “asynchronous” is borrowed from the cloud computing community [22]. In other words, the scale-up and dispatching processes are decoupled. The asynchronous approach takes scalability to the next level, for instance because it facilitates the deployment of systems with a large number of dispatchers [21], and is one principle underlying real systems such as Knative [1], a Kubernetes-based platform to deploy and manage modern serverless workloads that is used among others by Google Cloud Run; see Section 5.1 for further details. In addition, instead of focusing on a specific load balancing and auto-scaling strategy, our work will provide a framework to evaluate the impact of a general class of auto-scaling mechanisms that are up to the platform user to choose or design. This will be one advantage of our framework with respect to existing works because systems such as Knative leave the platform user with such control.

1.1 Contributions

We propose a Markovian framework for load balancing that includes asynchronous auto-scaling mechanisms. We refer to this framework as ‘Asynchronous Load Balancing and Auto-scaling’ (ALBA). ALBA is inspired by and tailored to serverless frameworks such as Knative; more details in Section 2. Two mechanisms drive dynamics in ALBA:

- i) a *dispatching rule*, or load balancing rule, which defines how jobs are dispatched among the set of active servers as they join the system, and
- ii) a *scaling rule*, which defines how the number of active servers scales up and down over time, possibly as a function of the current system state.

In agreement with existing implementations of serverless frameworks [22], we assume that dispatching and scaling rules operate *asynchronously*. This implies that the capacity scaling decisions are not taken at

the moments where jobs arrive and represents a key difference with respect to the existing approaches in the literature. The main motivation for us to consider an asynchronous architecture is to provide the first performance model and analysis of existing serverless platforms such as Knative. Their asynchronous structure enhances scalability as it facilitates operations in large systems with several dispatchers. The dispatching rules included in our framework are Power-of- d and Join-Below-Threshold- d (JBT- d) because they are commonly used in serverless frameworks [2]. A typical scale-down rule turns a server off only if it remains idle during an expiration window [22, 1]. This rule, also known as “delay-off” [15], is easy to implement and will be assumed within the proposed framework. In contrast, we do not impose any particular structure on scale-up rules as they are often defined by the user of the serverless platform. Since we have fixed the scale-down rule, in the following the term “scaling rule” will refer to a scale-up rule.

To the best of our knowledge, ALBA is the first framework that models the interplay between load balancing and auto-scaling asynchronously. Our key technical contributions hold under a general assumption on the structure of scaling rules, see Assumption 2, and are as follows:

- In Theorem 1, we prove a mean-field limit theorem that provides an accurate deterministic approximation of the sample paths of the finite-dimensional stochastic process underlying ALBA. This enables analytical tractability and allows one to study dynamics easily. For instance, given an arbitrary scaling rule, it may be used to estimate the resulting proportion of active servers, and thus the energy costs, in both the transient and stationary regimes. We prove Theorem 1 following the framework developed in [34, 8], which allows us to handle discontinuities of the drift function of the underlying Markov chain.
- In Theorem 2, we characterize the *fixed points* of the mean-field limit in terms of a set of non-linear equations and provide a simple necessary and sufficient condition on the scaling rule able to tell whether or not full service capacity will be needed to handle the incoming demand. Within Power-of- d , roughly speaking, there always exists a unique fixed point if the scaling rule is “nice”. Within JBT- d , however, this is not the case: to ensure uniqueness within a certain class of interesting scaling rules, it is necessary that the scaling rule has access to the number of servers containing exactly one job at any point in time (see Remark 1).
- When the mean demand exceeds the current service capacity, one may expect that a (strictly) positive scale-up rate at all times is enough to eventually drive the system to the reversed situation where capacity exceeds, or matches, demand. In Proposition 1, we provide a counterexample showing that this is not necessarily the case. In addition, the mean-field dynamics may converge to different fixed points, depending on the initial conditions. This poses the challenge of designing scaling rules able to drive dynamics to a desired fixed point regardless of the initial condition. This is addressed in our next contribution.
- In Theorem 3, we investigate how to design *fluid optimal* scaling rules: we provide a simple general condition ensuring that dynamics of the mean-field limit converge to “delay and relative energy optimality”. Following [26], this is a situation where the user-perceived delay and the relative energy wastage induced by idle servers vanish. We show that delay and relative energy optimality can only be achieved within JIQ, or equivalently JBT-0. The proposed condition suggests to scale up capacity if and only if the mean demand exceeds the overall rate at which servers become active *and* idle. From a practical standpoint, this requires the central controller to estimate the mean job arrival rate, which can be done via machine learning techniques, and to have access to the amount of both initializing, i.e., in set-up mode, and busy servers containing exactly one job. In existing serverless platforms, this information is easily accessible and implies only a constant communication overhead per job as in standard implementations of JIQ (see Remark 5). In addition, we find that being able to distinguish between busy servers with one or more jobs is *necessary* for fluid optimality (see Remark 3). This exposes a structural difference with respect to synchronous architectures. In fact, delay and relative energy optimality can be achieved even when JIQ is synchronized with the ad-hoc scale-up rule proposed in [26], which turns a server on if all active servers are busy upon job arrivals. In this respect, our contribution is to show that optimality can be achieved under broader conditions and also within asynchronous architectures. In existing serverless platforms, we stress that decentralized implementations of load balancing and auto-scaling mechanisms are indeed asynchronous.

While we show that fluid optimality can only hold within JIQ, we observe that this may not be the convenient choice within architectures with several dispatchers. In this case, an exact implementation of JIQ implies an expensive communication overhead per job and Power-of- d may be the way to go. A further advantage of Power-of- d with respect to JIQ or JBT- d is that is *stateless*, i.e., it does not require the dispatcher(s) to store information about the server states. This stateless feature is generally required for load balancing at the network layer [12]. Within these scenarios, the advantage of the proposed framework is to allow one to be able to design and efficiently evaluate the performance of different scaling rules. To the best of our knowledge, our work is the first to provide such ability.

As application of our results, we develop a tractable optimization framework allowing the system manager to trade off between performance and energy costs. The main purpose of this optimization framework is to illustrate how the results presented in this paper can be applied.

1.2 Organization

This paper is organized as follows. In Section 2, we build the ALBA framework and define the structure of the scaling rules considered in our framework. In Section 3, we present our main results: Theorems 1, 2 and 3. In Section 4, we show an application example of our results to trade off between energy and performance. In Section 5, we review the existing literature, and in Section 6, we draw the conclusions. Proofs of our main results are deferred to Appendix 7.

2 Asynchronous Load Balancing and Auto-scaling (ALBA)

In this section, we first describe the main principles at the basis of Asynchronous Load Balancing and Auto-scaling (ALBA). Since our aim is to develop a model tailored to serverless computing, we will make several references to Knative, a popular serverless framework for hosting Function-as-a-Service processing that is used, among others, by Google Cloud Run. Then, we propose two performance models for ALBA. The first captures the stochastic nature of the underlying dynamics while the second is deterministic and will serve to approximate the complex dynamics induced by the first. The advantage of the deterministic model is its tractability. Finally, we formalize the structure of the scaling rules investigated in this paper.

2.1 System Description

The proposed framework, ALBA, is composed of a system of N parallel servers, each with its own queue, that represent the nominal service capacity, i.e., the upper limit on the amount of resources that one user can have up and running at the same time¹. In the cloud computing community, servers are also referred to as containers, cloud functions, instances or replicas. Public serverless computing platforms usually require to specify such limit in order to ensure service availability for other users. In the following, the terms servers and queues will be used interchangeably. A server is said *warm* if turned on, *cold* if turned off and *initializing* if making the transition from cold to warm. These are the possible server states [41, 23, 22]. An initializing server performs basic startup operations such as connecting to database, loading libraries, etc. This is the time to provision a new function instance. Only warm servers are allowed to receive jobs. When no cold server exists, we say that the system is saturated; in ALBA, a saturated system is not representative of the average case. A server is also said *idle-on* if warm but not processing any job, and *busy* if warm and processing some job. Typically, billing policies charge per number of warm and initializing servers used per time unit.

Jobs join the system from an exogenous source to receive service. Upon arrival, each job is dispatched to a warm server according to some dispatching rule. After dispatching, each job is processed by the selected server according to the presumed scheduling discipline at that server. After processing, each job leaves the system.

Assumption 1. *Jobs are dispatched to servers according to either Power-of- d or Join-Below-Threshold- d (JBT- d).*

¹In Knative, this upper limit is specified by the `max-scale-limit` global key.

We recall that Power-of- d sends an incoming job to the shortest among $d \geq 1$ warm servers selected at random at the moment of its arrival and JBT- d sends an incoming job to a warm server containing no more than $d \geq 0$ jobs if one exists otherwise to a warm server selected at random. In all cases, ties are broken randomly. If $d = 0$, JBT- d is also known as Join-the-Idle-Queue (JIQ) [21]. We limit our framework to these types of schemes because they involve a constant communication overhead per job (in architectures with a single dispatcher) and because they are commonly used in practice. For instance, Knative uses Power-of-2 if no limit is set on the queue length of each server and JBT- d if such limit is set to d [2].

Alongside with the above job dynamics, the pools of warm/initializing/cold servers change over time in the background and in an asynchronous manner. Precisely, the platform monitors the system state at some epochs that we refer to as *scaling times*. At such times, a cold server is selected, provided that one exists, and becomes initializing according to the outcome of some scaling rule. After some *initialization time*, or coldstart latency, an initializing server becomes idle-on. When a server becomes idle-on, it becomes cold after a scale down delay, or *expiration time*, if during such time the server received no job; this scale-down rule is used in several serverless computing platforms (including Knative) [41, 38] and also in other settings [15]. Therefore, the decision of activating a warm server is taken by a central controller while the decision of making a server cold is taken by the server itself. We observe that the number of warm servers fluctuates from 0 to N over time. While in practice it may be possible to set a lower limit on the number of warm servers, the scale down to zero (or one) servers configuration is usually the default choice [3].

To a great extent, the scale up rule, the expiration rate and the scaling times are under the control of the platform user, which may design them in a way to optimize a trade-off between performance and energy. On the other hand, several measurements indicate that initialization times are typically one order of magnitude higher than jobs' service times in serverless platforms [22, 41].

2.2 Notation

We introduce some notation that will be used throughout the paper. Let $B \in \mathbb{Z}_+ \cup \{+\infty\}$ be a constant that will denote the buffer size of each server. We use $\mathbb{I}_{\{A\}}$ to denote the indicator function of A . If $a \in \mathbb{R}$ and A denotes an interval, $\mathbf{1}_A^a := \mathbb{I}_{\{a \in A\}}$. We also let $(\cdot)^+ := \max\{\cdot, 0\}$ and $\|\cdot\|$ denotes the L_1 norm. Unless specified otherwise, (i, j) ranges over the set $\{0, \dots, B\} \times \{0, 1, 2\}$ if $B < \infty$ and over $\mathbb{Z}_+ \times \{0, 1, 2\}$ otherwise. The process of interest will take values in

$$\mathcal{S} := \left\{ (x_{i,j} \in \mathbb{R}_+, \forall (i, j)) : \sum_{i,j} x_{i,j} = 1 \right\} \quad (1)$$

and our analysis holds under the distance function d_w induced by the weighted ℓ_2 norm $\|\cdot\|_w$ on $\mathbb{R}^{\mathbb{Z}_+}$ defined by $\|x - x'\|_w^2 := \sum_{i,j} \frac{|x_{i,j} - x'_{i,j}|^2}{2^{i+j}}$. For $x \in \mathcal{S}$, let $y_i := \sum_{k \geq i} x_{k,2}$. We also let $\mathcal{S}_1 := \{x \in \mathcal{S} : \sum_{i \geq 1} i x_{i,2} < \infty\}$.

2.3 Markov Model

We model the dynamics induced by ALBA in terms of a continuous time Markov chain. The exogenous arrival process of jobs is assumed to be Poisson with rate λN , with $0 < \lambda < 1$. Here, we may consider a time-varying arrival rate of the form $\Lambda(t)N$, where $\Lambda(t)$ is a bounded positive real-valued function, but we do not consider this case for simplicity. The processing times, or service times, of jobs are independent and exponentially distributed random variables with unit mean, and servers process jobs according to any work-conserving discipline. Upon arrival, each job is assigned to one of the available warm servers as specified in Assumption 1. In the extreme case where no warm server exists, we assume that the job is lost. We also assume that each server can contain at most $B > d$ jobs and a job that is sent to a server with B jobs is rejected. If not specified otherwise, B is either finite or infinite. At each scaling time, a cold server is selected uniformly at random, provided that one exists, and becomes initializing with some probability g , referred to as *scaling probability* (or rule), that will depend on the system state; in the Conclusions, we will discuss how our work adapts to the case where a random number of cold servers is selected at each scaling time. Given that jobs arrive with a rate proportional to N and only one server can be added at each scaling time, in our model we let the scaling frequency increase with N as well. As it occurs in Knative, this implies that the number of servers created in a time window of constant size is proportional to N if within such window the

scaling probability is not zero. We let the inter-scaling, initialization and expiration times be independent and exponentially distributed with rate αN , β and γ , respectively.

The five sequences of inter-arrival, service, inter-scaling, initialization and expiration times are also assumed mutually independent.

Let $Q^N(t) := (Q_1^N(t), \dots, Q_N^N(t))$ be the vector of queue lengths at time t , including the jobs in service, and let $S^N(t) := (S_1^N(t), \dots, S_N^N(t))$ be the vector of server states. Specifically, $S_k^N(t) \in \{0, 1, 2\}$ indicates whether server k is cold ($S_k^N(t) = 0$), initializing ($S_k^N(t) = 1$) or warm ($S_k^N(t) = 2$) at time t . Under the above assumptions, the stochastic process $(Q^N(t), S^N(t))$ is a continuous-time Markov chain on state space $\{(n, s) \in \{0, \dots, B\}^N \times \{0, 1, 2\}^N : n_k > 0 \Rightarrow s_k = 2, \forall k = 1, \dots, N\}$.

It is convenient to describe dynamics in terms of the process $X^N(t) := (X_{0,0}^N(t), X_{0,1}^N(t), X_{i,2}^N(t) : i = 0, \dots, B)$ where

$$X_{i,j}^N(t) := \frac{1}{N} \sum_{k=1}^N \mathbb{I}_{\{Q_k^N(t)=i, S_k^N(t)=j\}} \quad (2)$$

is the proportion of servers in state j with i jobs at time t . The process $X^N(t)$ is still a Markov chain with values in some set $\mathcal{S}^{(N)}$ that is a subset of \mathcal{S} . Let $e_{i,j} := (\delta_{i,i'} \delta_{j,j'} \in \{0, 1\} : i' \geq 0, j' = 0, 1, 2)$ where $\delta_{a,b}$ denotes the Kronecker delta and let $x := (x_{i,j}) \in \mathcal{S}^{(N)}$ denote a generic state of $X^N(t)$. For conciseness, the Markov chain $X^N(t)$ has the following transitions:

$$\begin{aligned} x \mapsto x' &:= x + \frac{1}{N}(e_{i,2} - e_{i-1,2}) && \text{with rate } \lambda N f_{i-1}(x) \\ x \mapsto x' &:= x + \frac{1}{N}(e_{i-1,2} - e_{i,2}) && \text{with rate } x_i N \\ x \mapsto x' &:= x + \frac{1}{N}(-e_{0,0}, e_{0,1}) && \text{with rate } \alpha N g \\ x \mapsto x' &:= x + \frac{1}{N}(-e_{0,1}, e_{0,2}) && \text{with rate } \beta x_{0,1} N \\ x \mapsto x' &:= x + \frac{1}{N}(e_{0,0} - e_{0,2}) && \text{with rate } \gamma x_{0,2} N \end{aligned}$$

for all $i = 1, \dots, B$, provided that $x, x' \in \mathcal{S}^{(N)}$. Here, $g := g(x) : \mathcal{S} \rightarrow [0, 1]$ is the scaling probability, and $f_i(x)$, which depends on the dispatching rule, represents the probability of assigning an incoming job to a warm server containing exactly i jobs. If $y_0 > 0$, within Power-of- d we have (assuming that server selections are with replacement)

$$f_i(x) = \frac{y_i^d - y_{i+1}^d}{y_0^d}, \quad i = 0, \dots, B-1 \quad (3)$$

where $y_i := y_i(x) := \sum_{j \geq i} x_{j,2}$, and within JBT- d we have

$$f_i(x) = \frac{x_{i,2} \mathbb{I}_{\{\sum_{k=0}^d x_{k,2}=0\}}}{y_0} + \frac{x_{i,2} \mathbb{I}_{\{\sum_{k=0}^d x_{k,2}>0\}}}{\sum_{k=0}^d x_{k,2}} \mathbb{I}_{\{i \leq d\}}, \quad i = 0, \dots, B-1 \quad (4)$$

where we have taken the convention that $0/0 = 0$. If $y_0 = 0$, then $f_i(x) = 0$ as no warm server exists.

2.4 Deterministic Model

We introduce the deterministic (or fluid, mean-field) model for the dynamics of ALBA.

Definition 1. A continuous function $x(t) : \mathbb{R}_+ \rightarrow \mathcal{S}$ is said to be a fluid model (or fluid solution) if for almost all $t \in [0, \infty)$

$$\dot{x}_{0,0} = \gamma x_{0,2} - \alpha g \mathbb{I}_{\{x_{0,0}>0\}} - \gamma x_{0,2} \mathbb{I}_{\{x_{0,0}=0, \gamma x_{0,2} \leq \alpha g\}} \quad (5a)$$

$$\dot{x}_{0,1} = \alpha g \mathbb{I}_{\{x_{0,0}>0\}} - \beta x_{0,1} + \gamma x_{0,2} \mathbb{I}_{\{x_{0,0}=0, \gamma x_{0,2} \leq \alpha g\}} \quad (5b)$$

$$\dot{x}_{0,2} = x_{1,2} - h_0(x) + \beta x_{0,1} - \gamma x_{0,2} \quad (5c)$$

$$\dot{x}_{i,2} = x_{i+1,2} \mathbb{I}_{\{i < B\}} - x_{i,2} + h_{i-1}(x) - h_i(x) \mathbb{I}_{\{i < B\}}, \quad i = 1, \dots, B \quad (5d)$$

where $g := g(x) : \mathcal{S} \rightarrow [0, 1]$, and

$$h_i(x) = \begin{cases} \lambda \frac{y_i^d - y_{i+1}^d}{y_0^d} & \text{if } y_0 > 0 \\ \min\{\beta x_{0,1}, \lambda\} & \text{otherwise} \end{cases} \quad (6)$$

if Power-of- d is applied, and

$$h_i(x) = \begin{cases} \lambda \frac{x_{i,2}}{\sum_{k=0}^d x_{k,2}} \mathbb{I}_{\{i \leq d\}} & \text{if } y_0 > 0, \sum_{k=0}^d x_{k,2} > 0 \\ (\beta x_{0,1} + x_{d+1,2} \mathbb{I}_{\{i=d\}}) \mathbb{I}_{\{x_{d+1,2} + (d+1)\beta x_{0,1} \leq \lambda\}} & \text{if } y_0 > 0, \sum_{k=0}^d x_{k,2} = 0, i \leq d, \\ \frac{x_{i,2}}{y_0} (\lambda - x_{d+1,2} - (d+1)\beta x_{0,1})^+ & \text{if } y_0 > 0, \sum_{k=0}^d x_{k,2} = 0, i > d, \\ \min\{\beta x_{0,1}, \lambda\} & \text{otherwise} \end{cases} \quad (7)$$

if JBT- d is applied.

As for $X_{i,j}^N(t)$, $x_{i,j}(t)$ is interpreted as the proportion of servers in state j with i jobs at time t .

Let us provide some intuition about the fluid model. First, when a strictly positive fluid mass of warm server exists, i.e., $y_0 > 0$, the functions h_i are interpreted as the rate at which jobs are assigned to servers with exactly i jobs. When the amount of fluid of cold servers is strictly positive, i.e., $x_{0,0} > 0$, to some extent these equations may be interpreted as the conditional expected change, or *drift*, from state x of the Markov chain $X^N(t)$. In contrast, when $x_{0,0} = 0$, there exists a term, $-\mathbb{I}_{\{x_{0,0}=0, \gamma x_{0,2} \leq \alpha g\}} \gamma x_{0,2}$ (see (5a) and (5b)), that still drains the amount of cold servers down. This is due to warm servers that become cold but immediately turn initializing and it appears if the scaling rule is ‘greedy enough’, i.e., if the rate at which new initializing servers can be created is greater than or equal to the rate at which warm servers go cold. This term is due to fluctuations of order $1/N$ that appear when $X_{0,0}^N(t) = 0$, which bring discontinuities in the drift of $X^N(t)$, and will come out from the stochastic analysis developed in Section 7.1.

Now, let us focus on (6) and (7), and let us assume that $y_0 > 0$. In the case of Power-of- d , $h_i = \lambda f_i$ and $x(t)$ evolves following the natural dynamics of Power-of- d as in [24], though normalized on the variable mass of warm servers $y_0(t)$. The case of JBT- d is more delicate because of the discontinuous structure of f_i in (4). If a strictly positive fraction of warm servers with no more than d jobs exist, then $h_i = \lambda f_i$ and $x(t)$ evolves following the natural dynamics of JBT- d , though again normalized on a variable number of servers. On the other hand, when $\sum_{k=0}^d x_{k,2} = 0$, there is a flow of warm servers with at most d jobs that are created but immediately used for dispatching jobs. Specifically, there are two factors that come into play here: the first is due to initializing servers that get warm with exactly i jobs (with rate $\beta x_{0,1}$), for all $i \leq d$, and the second is due service completions from servers with exactly $d+1$ jobs (with rate $x_{d+1,2}$). The resulting rate can not be greater than λ , the rate where jobs are assigned to servers, and this justifies the $\mathbb{I}_{\{x_{d+1,2} + (d+1)\beta x_{0,1} \leq \lambda\}}$ term. Then, the excess of such rate, $(\lambda - x_{d+1,2} - (d+1)\beta x_{0,1})^+$, is distributed uniformly over servers with $i > d$ jobs. In Theorem 3, we will show that such rate is key for the design of fluid optimal scaling rules. Finally, assume that no warm server exists, i.e., $y_0 = 0$. Here, initializing servers get idle-on with rate $\beta x_{0,1}$ but all of them are immediately filled by new arrivals if $\lambda \geq \beta x_{0,1}$, and in this case the mass of idle-on servers remains zero. Otherwise, $x_{0,2}$ increases with surplus rate $\beta x_{0,1} - \lambda$.

The existence of a fluid solution started in $x^{(0)} \in \mathcal{S}_1$ will be direct from Theorem 1.

2.5 Scaling Rules

The scaling rule g gives the probability to activate a new server at each scaling time as a function of the system state. The following assumption, which will hold throughout the paper, provides the structure of the scaling rules investigated in this paper.

Assumption 2. *The scaling rule $g : \mathcal{S} \rightarrow [0, 1]$ is Lipschitz continuous, and $g(x) > 0$ if $x_{0,0} = 1$.*

The last technical condition is natural and will rule out the existence of degenerate fixed points. We allow $g(x)$ to be greater than zero even when no cold server exists, i.e., $x_{0,0} = 0$. While this has no impact on the dynamics of the stochastic model, it does affect the fluid model as there may exist a flow of idle-on servers that go cold but instantly turn initializing keeping the proportion of cold servers at zero. This situation can occur if λ is large enough and not only in the transient regime; see Theorem 2.

We propose two scaling rules that satisfy Assumption 2 and that will be used for illustration purposes.

Definition 2. At each scaling time, if the system state is x ,

- Blind- θ activates a new server with probability $g(x) = \theta$, $\theta \in (0, 1]$;
- Rate-Idle activates a new server with probability $g(x) = \frac{1}{\lambda}(\lambda - \beta x_{0,1} - x_{1,2})^+$.

Blind- θ is oblivious of the system state and thus highly scalable. On the other hand, within Rate-Idle, the auto-scaler needs to know the amount of initializing servers, the amount of busy servers with exactly one job at any point in time and both the job arrival and server initialization rates, which can be easily estimated. If $\lambda > \beta x_{0,1} + x_{1,2}$, then the interpretation is that the scaling probability is proportional to the difference between the mean demand, λ , and the rate at which servers become idle-on, $\beta x_{0,1} + x_{1,2}$. Otherwise, the scale-up process is turned off. Rate-Idle is interesting because it will induce fluid optimality if combined with JIQ; see Theorem 3.

3 Main Results

In this section, we present our main results. First, in Theorem 1 we justify the use of the deterministic model to approximate the behavior of the stochastic. Then, we focus on properties of the deterministic model: we characterize its fixed points in Theorem 2 and investigate the design of optimal scaling rules in Theorem 3.

3.1 Connection between the Fluid and the Markov models

The following result shows that the fluid model can be seen as a first-order approximation of the sample paths of the stochastic.

Theorem 1. Let $T < \infty$, $x^{(0)} \in \mathcal{S}_1$ and assume that $\|X^N(0) - x^{(0)}\|_w \rightarrow 0$ almost surely. Then, limit points of the stochastic process $(X^N(t))_{t \in [0, T]}$ exist and almost surely satisfy the conditions that define a fluid solution started at $x^{(0)}$.

Proof. Given in Appendix 7. □

The stochastic and the deterministic models have some non-standard aspects that prevent us to prove Theorem 1 by directly applying Kurtz's theorem or similar known results. Specifically, the technical issues are that the trajectories of the deterministic model may cross or converge, as time increases, to points of discontinuity of its drift function and that buffer sizes are allowed to be infinite. To handle these issues, we follow the general framework in [34, 8] developing ad-hoc arguments specific to the structure of our problem.

In view of Theorem 1 and since typical and default maximum scale limit values are 1000 or more, i.e., $N \geq 10^3$, we expect that the fluid model $x(t)$ provides an accurate approximation of the average behavior of $X^N(t)$. To support this claim, we now present the results of numerical simulations; see also Section 4. Figure 1 (left) plots some trajectories of $x(t)$ and $X^N(t)$ when $N = 10^3$ and $B = 10^2$ along the coordinates of cold ($x_{0,0}$), initializing ($x_{0,1}$), idle-on ($x_{0,2}$) and busy (y_1) servers. Also, Figure 1 (right) plots the average number of jobs per warm server, which in state x is given by $Q(x) := \frac{1}{y_0} \sum_{i \geq 1} i x_{i,2}$. The fluid (stochastic) trajectories are always represented by dashed (continuous) lines and each curve is the average of ten simulations. Each simulation is based on 10^6 events. We have also set $\lambda = 0.7$, $\alpha = 0.05$, $\beta = 0.1$ and $\gamma = 0.025$. If a time unit is 10 milliseconds, these are realistic choices [22, 10]. As scaling rule, we have chosen Blind- θ where $\theta = \frac{0.5}{\alpha} \frac{1-\lambda}{\beta+1}$; this choice will ensure that a strictly positive proportion of cold servers exists in the long run (see Theorem 2). As dispatching algorithm, we have used Power-of- d with $d = 1$. At time zero, we have assumed that the system is minimally dimensioned for the average demand, i.e., $(1 - \lambda)N$ servers are cold and the remaining ones are idle-on. In both pictures, we observe that the fluid model captures the dynamics of $X^N(t)$ accurately.

Let us provide some intuition about the dynamics in Figure 1. Initially, the system is close to instability as capacity exactly matches demand. Here, $Q(x(t))$ increases rapidly and as soon as a warm server is created, it is filled with a job and as a result the proportion of idle-on servers decreases. There is also another factor that makes the number of idle-on servers decrease: Power-of- d , with $d = 1$, is not so powerful in discovering idle-on servers because a fraction of them go cold even in heavy load. This explains why the number of cold

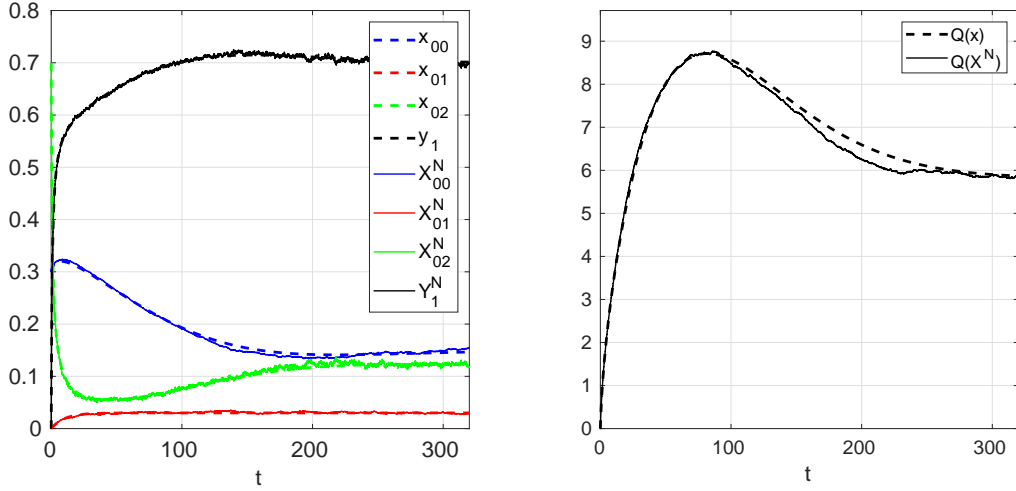


Figure 1: Numerical convergence of the stochastic model $X^N(t)$ (continuous lines), $N = 10^3$, to the fluid model $x(t)$ (dashed lines) when combining Power-of- d with $d = 1$ and Blind- θ .

servers (the blues lines) is increasing at the beginning. Then, more warm servers are created to mitigate the effect of the “close to instability” window on the accumulated overall number of jobs. Here, the mass of busy servers (y_1) becomes greater than the average demand $\lambda = 0.7$ and $Q(x(t))$ decreases. Finally, dynamics stabilize and in equilibrium there is a strictly positive fraction of servers that remain cold, initializing and idle-on. This indicates that there is a flux of idle-on servers that expires continuously even in equilibrium.

3.2 Characterization of Fixed Points

Theorem 1 justifies the use of the fluid model $x(t)$ to approximate the behavior of the stochastic model $X^N(t)$. We now investigate properties of the fluid model and in particular its fixed points when buffer sizes are infinite. The fluid model has the form $\dot{x} = F(x)$; see Definition 1. We say that $x^* \in \mathcal{S}_1$ is a *fixed point* if $F(x^*) = 0$. Now, for $x \in \mathcal{S}_1$, let us define the following conditions:

$$x_{0,0} + x_{0,1} + x_{0,2} + \lambda = 1 \quad (8a)$$

$$\beta x_{0,1} = \gamma x_{0,2} \quad (8b)$$

$$\gamma x_{0,2} \leq \alpha g(x), \quad \text{if } x_{0,0} = 0 \quad (8c)$$

$$\gamma x_{0,2} = \alpha g(x), \quad \text{if } x_{0,0} > 0 \quad (8d)$$

$$\text{if Power-of-}d \text{ is used: } x_{i,2} = (\lambda + x_{0,2}) \left(\left(\frac{\lambda}{\lambda + x_{0,2}} \right)^{\frac{d^i - 1}{d-1}} - \left(\frac{\lambda}{\lambda + x_{0,2}} \right)^{\frac{d^{i+1} - 1}{d-1}} \right), \quad i \geq 1 \quad (8e)$$

$$\text{if JBT-}d \text{ is used: if } x_{0,2} = 0: \quad x_{i,2} = 0, \quad 0 \leq i \leq d \quad (8f)$$

$$x_{d+i,2} = x_{d+1,2} \left(1 - \frac{x_{d+1,2}}{\lambda} \right)^{i-1}, \quad i \geq 2 \quad (8g)$$

$$x_{d+1,2} \in (0, \lambda] \quad (8h)$$

$$g(x) = 0 \quad (8i)$$

$$\text{if } x_{0,2} > 0: \quad x_{i,2} = \left(\frac{\lambda}{z_d + x_{0,2}} \right)^i x_{0,2} \mathbb{I}_{\{1 \leq i \leq d+1\}}, \quad i \geq 1 \quad (8j)$$

with $z_d \in [0, 1]$ being the unique solution of

$$z_d + x_{0,2} = \frac{1 - \left(\frac{\lambda}{z_d + x_{0,2}} \right)^{d+1}}{1 - \frac{\lambda}{z_d + x_{0,2}}} x_{0,2} \quad (9)$$

if $d \geq 1$ and $z_d = 0$ if $d = 0$. Here, z_d is interpreted as the proportion of busy servers with no more than d jobs. Let us also introduce the following assumption.

Assumption 3. For any $x_{0,2} \in [0, 1 - \lambda]$, (8e)-(8j) uniquely determine $x_{i,2}$ for all $i \geq 1$.

Within Power-of- d , this assumption is clearly satisfied by (8e). Within JBT- d , it is satisfied only if $x_{0,2} > 0$, as if $x_{0,2} = 0$, then $x_{d+1,2}$ is only required to belong to $(0, \lambda]$. Under Assumption 3, let $x^\circ = (x_{i,j}^\circ)$ be the unique point in \mathcal{S}_1 such that $x_{0,0}^\circ = 0$, $x_{0,1}^\circ = \frac{\gamma}{\beta+\gamma}(1 - \lambda)$, $x_{0,2}^\circ = \frac{\beta}{\beta+\gamma}(1 - \lambda)$.

The following result characterizes fixed points and provides a framework to evaluate the equilibrium fluid performance induced by generic scaling rules; see Section 7.2 for a proof.

Theorem 2. If $x^* \in \mathcal{S}_1$ satisfies the conditions in (8)-(9), then it is a fixed point of the fluid model with $B = +\infty$. In addition, under Assumption 3

1. $x_{0,0}^* > 0$ if and only if

$$\alpha g(x^\circ) < \frac{1 - \lambda}{\frac{1}{\beta} + \frac{1}{\gamma}}. \quad (10)$$

2. If (10) does not hold, then x° is the unique fixed point.

Proof. Given in Appendix 7. □

At the fluid scale and in a fixed point, Theorem 2 also provides the boundary scaling probability that distinguishes between a saturated and a non-saturated system. Specifically, if $g(x^\circ)$ does not satisfy (10), then no cold server exists in a fixed point but we observe that (8a) and (8b) imply that a strictly positive fraction of servers remain initializing, $\frac{\gamma}{\beta+\gamma}(1 - \lambda)$. The interpretation is that there is a mass of idle-on servers that go cold but instantly become initializing. This corresponds to a waste of resources because initializing servers cannot process jobs. In other words, a better performance may be obtained by keeping the initializing servers warm at all times (no auto-scaling); recall also that billing policies charge warm and initializing servers. If $g(x^\circ)$ satisfies (10), then in a fixed point there still exists a fraction of idle-on servers that go cold and instantly become initializing, provided that $g(x^\circ) > 0$. However, the pool of cold servers remains non-empty and this may give a benefit in terms of performance versus operational cost tradeoffs because cold servers are not charged.

Within Blind- θ , $g(x) = \theta$ and the conditions (8)-(9) easily identify a unique fixed point, say x^* , with $(x_{0,0}^*, x_{0,1}^*, x_{0,2}^*)$ not depending on the choice of the load balancing algorithm. The following remark says that uniqueness is not always guaranteed.

Remark 1 (Multiple Fixed Points). Suppose that $g(x) = 0$ whenever $y_1 = \lambda = 1 - x_{0,0}$ and that JBT- d is used. Then, Theorem 2 implies that uncountably many fixed points exist. In fact, while $x_{i,2} = 0$ for all $i = 0, \dots, d$ and $x_{i,2}$ is uniquely determined for all $i \geq d + 2$ once fixed $x_{d+1,2}$, the conditions (8)-(9) do not tie $x_{d+1,2} \in (0, \lambda]$ to a specific value.

3.2.1 Blind- θ and Random Dispatching

For illustration purposes, let us consider Blind- θ with random dispatching (Power-of-1). This combination does not involve any communication overhead among the auto-scaler, dispatchers and servers, and for this reason it is well suited for large systems with vast numbers of dispatchers. Here, Theorem 2 identifies a unique fixed point, x^* . After some algebra, we obtain $x_{0,2}^* = \min \left\{ \frac{\alpha\theta}{\gamma}, x_{0,2}^\circ \right\}$ and for the mean queue length per warm server, $Q(x) = \frac{1}{y_0} \sum_i i x_{i,2}$, we obtain (using also (8e))

$$Q(x^*) = \frac{\lambda}{\min \left\{ \frac{\alpha\theta}{\gamma}, x_{0,2}^\circ \right\}}. \quad (11)$$

As long as a strictly positive fraction of cold servers exists, or equivalently $\frac{\alpha\theta}{\gamma} < x_{0,2}^\circ$, we remark that $Q(x^*)$ grows linearly in λ .

3.3 Convergence to Multiple Fixed Points

As in the theory of dynamic systems, one is typically interested in whether or not any fluid solution $x(t)$ converges to x^* , as $t \rightarrow \infty$, regardless of the initial condition $x(0)$ and provided that x^* is the unique fixed point. In this case, x^* is called “global attractor”. Unfortunately, we have already shown in Remark 1 that uniqueness of a fixed point is not always guaranteed. To guarantee uniqueness, the following proposition shows that *it is not enough, as one may expect, to have a strictly positive scaling probability whenever the current capacity of warm servers is less than the average demand*, i.e., $g(x) > 0$ whenever $y_0 < \lambda$.

Let

$$\mathcal{S}_{\text{subopt}} := \{x \in \mathcal{S} : x_{0,0} = 1 - \lambda, x_{0,1} = x_{0,2} = 0, x_{1,2} < \lambda \text{ and (8g) holds with } d = 0\} \quad (12)$$

and let $\bar{Q}(x) := \sum_{i \geq 1} ix_{i,2}$ denote the average number of jobs per server in state $x \in \mathcal{S}$; here, cold and initializing servers are included in the counting.

Proposition 1. *Let $g(x)$ be any scaling rule such that*

$$g(x) = \frac{1}{\lambda}(x_{0,0} - 1 + \lambda)^+, \quad \forall x \in \mathcal{S} : y_0 < \lambda. \quad (13)$$

Let $x(t)$ denote a fluid model induced by such $g(x)$ and JIQ such that

$$x_{0,0}(0) > 1 - \lambda, x_{0,2}(0) = 0, x_{1,2}(0) + \beta x_{0,1}(0) < \lambda < \bar{Q}(x(0)) < \infty. \quad (14)$$

Suppose that $\beta < 1$, $\alpha \neq \beta$ and $B = +\infty$. Then,

$$g(x(t)) > 0, \quad \forall t \geq 0 \quad (15)$$

$$\lim_{t \rightarrow \infty} \bar{Q}(x(t)) = \bar{Q}(x(0)) + \frac{\alpha + \beta}{\alpha\beta}(x_{0,0}(0) - 1 + \lambda) + \frac{x_{0,1}(0)}{\beta} > \lambda. \quad (16)$$

In addition, $y_0(t) \uparrow \lambda$, and if $x_{1,2}(t) \rightarrow x_{1,2}(\infty)$, then $x(t) \rightarrow x(\infty)$ with $x(\infty) \in \mathcal{S}_{\text{subopt}}$.

Proof. Given in the Appendix. □

Thus, while the proportion of warm servers converges to λ , such convergence may occur *from below* even if there always exists a strictly positive probability of creating new warm servers. In this case, the average demand is greater than the current service capacity at any point in time and this makes the mean queue length converge to a limit that depends on the initial conditions.

Let us comment a little bit further and prepare the setting for our next contribution. To create the underload situation above where $y_0(t) \uparrow \lambda$, it is not necessary to assume that all warm servers are initially busy ($x_{0,2}(0) = 0$), though we have included this condition in (14) to simplify our proof. In contrast, to avoid this situation, it may be sufficient that $g(x)$ is bounded away from zero whenever $y_0 < \lambda$. By continuity, this implies that $g(x) > 0$ as well whenever $y_0 = \lambda$, but in this case the resulting scaling rule will not possess the optimality property stated in Theorem 3 below (as this will imply that $g(x^*) > 0$). On the other hand, one may consider a scaling rule that is discontinuous on the set $\{x : y_1 = \lambda\}$, a setting that does not satisfy Assumption 2. Here, beyond revisiting Theorem 1 for justification of the fluid model, the problem is that scale-up decisions would significantly depend on small perturbations of the equilibrium system state, severely impacting robustness from a practical standpoint.

3.4 Optimal (Stable) Design

Within Blind- θ , Theorem 2 guarantees the existence of a unique fixed point, say x^* , and all of our numerical simulations, which we omit, indicate that it is a global attractor. Here, necessarily $x_{0,2}^* > 0$, by (8d), which means that a number of warm servers remain idle-on in equilibrium. Clearly, this is not optimal for energy consumption because idle-on servers consume energy. While it is mathematically interesting to find conditions on the scaling rule that imply the existence of a global attractor, our goal here is more ambitious: we are interested in how to drive the limit behavior of any fluid solution $x(t)$ to the *optimal* point $x^* \in \mathcal{S}$, uniquely defined by $x_{0,0}^* = 1 - \lambda$ and $x_{1,2}^* = \lambda$, regardless of its initial condition $x(0) \in \mathcal{S}_1$.

Remark 2 (Fluid Optimality). *Following [26], in x^* dynamics have achieved “delay and relative energy optimality” in the sense that both the waiting time of jobs and the relative energy portion consumed by idle-on and initializing servers vanish in the limit. Here, a possible intuition is that each job is always assigned to a busy server with exactly one job but at the precise moment where it completes the processing of its previous job. Therefore, service capacity perfectly matches demand.*

A direct consequence of Theorem 2 and (8d) is that it is necessary to impose $g(x^*) = 0$ to achieve fluid optimality. Within Power-of- d , this is impossible as this condition would imply that $x_{0,2} = 0$, and then (8e) would imply $x_{i,2} = 0$ for all i , contradicting that $\|x\| = 1$. In fact, Theorem 2 implies that the unique candidate is JIQ, though it leaves open the possibility that $x(t)$ may converge to a fixed point in the sub-optimal set $\mathcal{S}_{\text{subopt}}$, see (12). Thus, it remains to understand what additional structure the scaling rule $g(x)$ should satisfy to make x^* a global attractor. Here, we observe that Remark 1 suggests that even the knowledge of the amount of busy servers is not enough. More precisely, it implies that one needs $g(x) > 0$ for all $x \in \mathcal{S}_{\text{subopt}}$ as otherwise multiple fixed points exist. Therefore, given the structure of $\mathcal{S}_{\text{subopt}}$ and x^* , we have the following remark.

Remark 3. *A fluid optimal scaling rule needs the access to the amount of busy servers with exactly one job, i.e., $x_{1,2}$.*

The following result provides a general condition that yields fluid optimality.

Theorem 3 (Optimal Design). *Let $\beta < 1$ and let $x(t)$, with $x(0) \in \mathcal{S}_1$, denote a fluid solution induced by JIQ and any scaling rule $g(x)$ that satisfies, beyond Assumption 2,*

$$g(x) = 0 \text{ if and only if } x_{1,2} + \beta x_{0,1} \geq \lambda. \quad (17)$$

Then, $\lim_{t \rightarrow \infty} \|x(t) - x^\|_w = 0$.*

The key observation is that $x_{1,2} + \beta x_{0,1}$ is interpreted as the overall rate at which servers become idle-on. Thus, our requirement for the design of an optimal scaling rule is to ensure to scale up resources whenever the excess of the mean demand over the rate at which servers become idle-on is positive, as in this case JIQ is powerful enough to fill them up immediately saturating the surplus service capacity. Otherwise, the scale-up process is turned off ($g = 0$), and in this case the natural dynamics induced by both JIQ and the scale-down rule are enough to drive the system behavior to the desirable configuration x^* .

Remark 4. *Rate-Idle, see Definition 2, satisfies (17).*

As discussed in Section 2.1, the assumption $\beta < 1$, i.e., the mean server initialization rate is smaller than the mean job service rate, is largely accepted in practice [22, 41]. From a mathematical standpoint, it is not necessary for fluid optimality but simplifies our proof.

Remark 5 (Communication Overhead). *A scaling rule satisfying (17) requires the central controller to have access to the amount of initializing and busy servers containing exactly one job, i.e., $x_{0,1}$ and $x_{1,2}$. Since an initializing server informs the platform as soon as it becomes warm, $x_{0,1}$ is easily obtained in practice. For $x_{1,2}$, the auto-scaler can run a local memory with N slots, where the n -th slot indicates the state of server n , say ‘Cold’, ‘Init’, ‘Idle-on’, ‘Busy₁’ and ‘Busy_{≥2}’, with obvious interpretations. Then, one way to update the memory is by letting each server send a message to the auto-scaler whenever the transitions ‘Busy_{≥2}’ \rightarrow ‘Busy₁’, ‘Busy₁’ \rightarrow ‘Idle-on’ and ‘Idle-on’ \rightarrow ‘Busy₁’ occur. As in standard implementations of JIQ, this involves only a constant number of messages per job to be exchanged between the auto-scaler and the servers.*

Finally, the condition (17) is general enough to provide the platform user with some flexibility when designing an optimal scaling rule. This opens the way to a new level of optimizations as discussed in the next section.

4 Energy Optimization with Performance Guarantees

Given that the fluid model provides a tractable first-order approximation of the stochastic dynamics within ALBA and that we have considered mild assumptions on the structure of scaling rules (Assumption 2), it is

natural to use the fluid model in an optimization framework to trade off between performance and energy costs. As proof of concept, the objective of this section is to show a high-level application of our results that may serve as a base for future more sophisticated techniques, which may integrate machine learning mechanisms or consider switching costs.

We limit the focus on JIQ and on sets of scaling rules that satisfy the assumptions in Theorem 3, say \mathcal{G} , as they automatically imply fluid optimality (Remark 2) in the *stationary* regime. Let us define the cost function \mathcal{J}_g as the long-run time average of a linear combination between the power consumption $P(x) = c_{0,1}x_{0,1} + c_{0,2}x_{0,2} + c_{1,2}y_1$, $c_{i,j} > 0$, and the average queue length per busy server $Q(x) = \frac{1}{y_1} \sum_i ix_{i,2}$ induced by the scaling rule g (as in, e.g., [4]), i.e.,

$$\mathcal{J}_g := \lim_{T \rightarrow \infty} \frac{1}{T} \int_0^T (\kappa_1 P(x(t)) + \kappa_2 Q(x(t))) dt \quad (18)$$

where $\kappa_i \geq 0$, $i = 1, 2$; one can think κ_1 in terms of \$/watt and κ_2 in terms of \$/job. Then, Theorem 3 implies that

$$\inf_g \mathcal{J}_g = \mathcal{J}_{g^*} = \kappa_1 P(x^*) + \kappa_2 Q(x^*) = \kappa_1 c_{1,2} \lambda + \kappa_2, \quad \forall g^* \in \mathcal{G}. \quad (19)$$

While all policies in \mathcal{G} yield the same (optimal) cost, their behavior is clearly different trajectory-wise. Depending on the application, a platform user has several options to single out a policy in \mathcal{G} that satisfies a further level of optimization. For instance, a substantial portion of the applications hosted in cloud networks have ultra-low delay requirements, as this may have important consequences on e-commerce sales. On the other hand, also energy bills are equally important from both financial and environmental standpoints. Here, a system manager may want to look for a scaling rule in \mathcal{G} such that

$$Q(x(t)) \leq q, \quad \forall t \geq 0 \quad (20)$$

where q is related to the desired user-perceived performance guarantee; by Little's law, (20) is equivalent to a constraint on the mean response time. Towards this purpose, the parameterized subset of scaling rules taking the form

$$g(x) = \frac{1 - \exp(-\frac{\eta}{\lambda}(\lambda - x_{1,2} - \beta x_{0,1})^+)}{1 - \exp(-\eta)}, \quad \eta > 0, \quad (21)$$

may be considered. Note that these satisfy both Assumption 2 and (17), that Rate-Idle is recovered when $\eta \downarrow 0$, and that $g(x) = \mathbb{I}_{\{\lambda \geq x_{1,2} + \beta x_{0,1}\}}$ when $\eta \rightarrow \infty$. The control parameter $\eta > 0$ indicates how aggressive the scaling rule is. This provides intuition for considering scaling rule of the form in (21). Then, the goal is to find η such that (20) holds true, provided that one exists. This problem can be easily addressed numerically within the proposed deterministic model. Assume that the system is currently in a light-load condition, say $\lambda = 0.25$, and that, as a result, it is dimensioned accordingly to save energy, say $x_{0,0} = 1 - \lambda - 0.05$, with $x_{0,2} = 0.05$ and $x_{1,2} = \lambda$; the extra 0.05 is meant to keep a reserve of idle-on servers ready to go. Then, at time zero, an unexpected workload peak occurs, and $\lambda = 0.5$. Here, the platform needs to automatically adjust the service capacity while ensuring (20). Let us assume $q = 2$, $\alpha = 0.35$, $\beta = 0.1$ and $\gamma = 0.025$. The dashed lines in Figure 2 represent the dynamics of the fluid queue lengths $Q(x(t))$ and scaling probabilities $g(x(t))$, for $\eta = 1, 10^3$. The corresponding continuous lines represent the average of ten simulations of the stochastic model $X^N(t)$ with $N = 1000$. First, let us remark that the fluid model approximation accurately captures the dynamics of $X^N(t)$, though it slightly underestimates queue lengths and scaling probabilities. Now, let us consider $\eta = 1$. Initially, queue lengths increase as expected due to the surge of demand and the scaling probability is large enough to drive the proportion of cold servers to zero. This explains the non-differentiability point of the trajectory of the scaling rule because the amount of initializing servers stops to grow. Then, the system has enough capacity to drain the load and at some point the rate at which servers become idle-on overflows the mean demand, i.e., $x_{1,2} + \beta x_{0,1} > \lambda$, so that eventually $g(x(t)) = 0$. Finally, queue lengths assess to their asymptotic value $Q(x^*) = 1$. We conclude that $\eta = 1$ is enough to make (20) holds true. We also notice that the choice $\eta = 10^3$, which essentially means to scale up resources at the maximum available rate α whenever $x_{1,2} + \beta x_{0,1} < \lambda$, has little impact on performance. Nonetheless, it should be clear that the larger the value of η , the larger the resulting time-average power consumption. A deeper analysis is out of the scope of the present work.

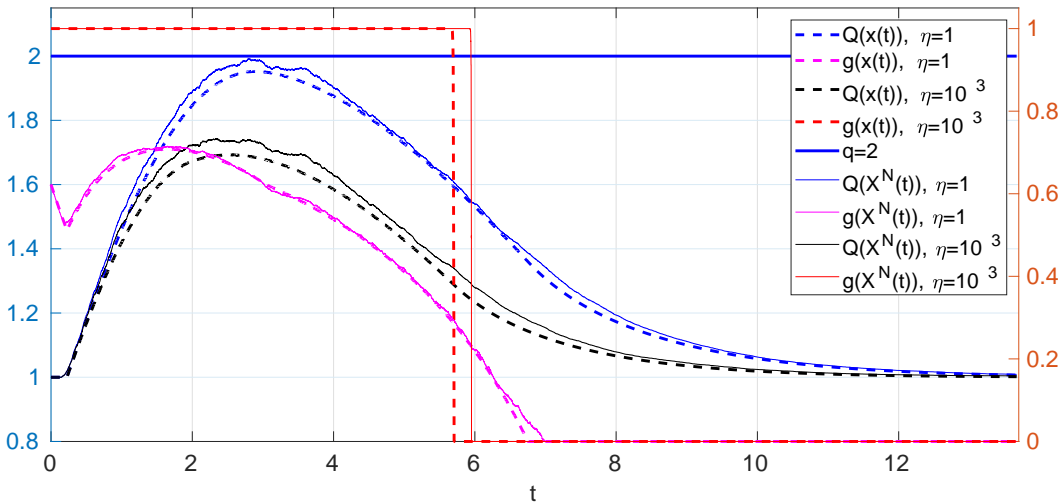


Figure 2: Transient behavior of the queue lengths and scaling probabilities by varying η , see (21), for the both the fluid ($x(t)$) and stochastic ($X^N(t)$) models with $N = 1000$.

5 Literature Review

The existing literature related to load balancing and auto-scaling is huge and our goal here is to provide the necessary background highlighting the difference with respect to our work.

The most popular examples of load balancing techniques that work well when servers are homogeneous, i.e., all servers have the same processing speed, are Random, Round-Robin (RR) [20], Power-of- d [24], Join-the-Idle-Queue (JIQ) [21], Least-Left-Workload (LLW) and Size Interval Task Allocation (SITA) [19, 18]. Random sends each job to random server, RR sends jobs to servers in a cyclic manner, Power-of- d sends an incoming job to the least loaded server among d selected uniformly at random. JIQ sends an incoming job to a random idle server if an idle server exists and to a random one otherwise, LLW sends an incoming jobs to the queue having the shortest workload, and SITA sends a job to a given server if its size belong to a given interval. In all cases, ties are broken randomly. In general, it is not possible to identify which of these algorithms is the best because the general answer depends on the underlying architecture, load conditions, service time distribution and on the amount of information available to the dispatcher [37]. Recently, a number of works attempted to understand under which conditions the mean waiting time can be driven down to zero in the mean field limit, i.e., in the limiting regime where the arrival rate grows linearly with the number of servers while keeping the average load below one. It has been shown that this is possible within different load balancing algorithms and architectures. Examples include JIQ [32], Power-of- d with $d \rightarrow \infty$ as the network size grows to infinity [25], Power-of- d with memory [6], SITA combined with RR [5] and the pull-based policies developed in [13, 36]. To some extent, the fundamental limits of load balancing are described in [13], where the authors investigate trade-offs between performance, communication overhead and memory within a certain class of symmetric architectures. There are several variants and generalization of the above algorithms and these are meant to handle i) heterogeneous servers [33, 9], ii) multiple dispatchers [35, 33], iii) increased information to the dispatcher [17, 6], or iv) the case where model parameters such as arrival and service rates are unknown [7].

The dynamics of the above dispatching algorithms have been analyzed under the assumption that jobs are dispatched among a *constant* number of parallel servers. To the best of our knowledge, the only exceptions are [26, 16], which provide the first performance model where load balancing and auto-scaling operate jointly within the same timescale. Here, JIQ is combined with a specific scaling strategy that turns a server off if that server remains idle for a certain amount of time, and turns a server on at the moment of a job arrival if all active servers are busy upon arrival of that job. In a regime where the traffic demand and nominal service capacity grow large in proportion, this mechanism yields zero user-perceived delay as in the classical

version of JIQ with no auto-scaling [32] but also deactivates any surplus idle servers, ensuring that the relative energy wastage vanishes in the limit as well. In this sense, this strategy induces asymptotic *delay and relative energy optimality*. These properties have been strengthened in [27], where the authors relax some finite buffer assumptions.

Let us comment on the differences between our work and [26, 16]. First, while in these references the load balancing and auto-scaling processes are *synchronous*, in our framework they operate *asynchronously*; see below for more details about the synchronous and asynchronous approach. Second, we do not focus on a specific load balancing and auto-scaling strategy: our framework allows for the design of general scaling rules (see Assumption 2) and considers a wide class of load balancing schemes that is not limited to JIQ. In fact, Power-of- d may be the best option when the underlying architecture is composed of multiple dispatchers because it still involves a constant communication overhead per job, which is not the case within JIQ. Third, we show that delay and relative energy optimality can be achieved under broad assumptions (see Theorem 3). In turn, these yield the definition of optimization frameworks allowing the system manager to further trade off between energy and performance according to his needs.

Another reference that is close to our work is [22], where the authors propose a performance model for auto-scaling that is tailored to the serverless computing platform AWS Lambda. Here, the auto-scaling strategy is similar to [26] in the sense that it is synchronized with job arrivals but different because an incoming job that finds all servers busy is sent anyway, after a coldstart latency, to an idle server that is turned on at the moment of its arrival. If this is not possible because no further server is available, then the job is rejected. Within this approach, there is no queueing because jobs are always assigned to idle servers.

We also mention [11], where the authors propose a synchronous and decentralized approach that is a hybrid between [22] and [26]. Upon arrival, a job visit the active servers in a sequential order until a idle one is met. This server will process the job if such server exists, otherwise the job queues up in the last active server and this situation triggers a scale-up decision if the number of jobs in such queue overflows a given threshold. This architecture is meant to operate entirely within the network layer (Layer 4) using IPv6 Segment Routing. As in [22], their performance analysis assumes a timescale separation between the load balancing and auto-scaling processes.

There is a line of research works developing performance models for auto-scaling in a different vein. One approach that has been widely considered in the literature is based on the assumption that jobs join a global queue before being dispatched to one out of a number of parallel servers. This type of approach yields models that are variations of M/M/K or M/M/K/N queues [15, 43, 28, 4]. In contrast, the focus of this paper is on decentralized architectures where each server has its own queue, which enhance scalability. A further class of performance models for auto-scaling in cloud systems assume that job dynamics reach stochastic equilibrium between consecutive changes of the overall processing capacity [39, 31]; see also Section 8.4 in [29]. This approach is arguable in the context of serverless computing platforms because the auto-scaling process operates at a fast timescale [40, 41, 22]. Finally, we mention that auto-scaling can be performed at the level of a single centralized processor. This type of auto-scaling is referred to as “speed scaling” [42, 4].

5.1 Synchronous vs Asynchronous in Serverless Computing

The load balancing and auto-scaling processes of existing implementations of public serverless computing platforms can be “synchronous” or “asynchronous”; this terminology is borrowed from the cloud computing community [22].

- In platforms such as AWS Lambda, Azure Functions, IBM Cloud Functions and Apache OpenWhisk, a new server (instance) is turned on at the arrival time of a job if the job itself finds all servers busy [30, 41]. Then, once the server is turned on, the job is executed on that server. The extra time that an incoming job may incur if it finds all servers busy (usually referred to as coldstart latency [22]) can pay off because of the order of 10^2 milliseconds [41]. Sporadic excesses of such duration are acceptable for a substantial number of applications hosted in these systems. Within these technologies, the auto-scaling process is thus *synchronized* with job arrival and dispatching decision times, and all the above implementations require the incoming jobs to wait in a *central* queue before dispatching. This type of auto-scaling is also referred to as *scale-per-request* [22].
- In platforms such as Google Cloud Run and Knative, the load balancing and auto-scaling processes

are decoupled in the sense that servers are turned on *asynchronously* at certain user-defined scaling times. Specifically, upon arrival, a job is immediately dispatched to some running server according to some load balancing algorithm such as Power-of- d [2]. Independently of this, the auto-scaling process decides whether the current processing capacity should increase as a function of user-defined metrics, or scaling rules, that may depend on instantaneous observations of the current system state. Because of this decoupling, jobs may be assigned to busy servers. Asynchronous implementations of serverless platforms such as Knative are *decentralized*, i.e., each server has its own queue, and thus highly scalable. This type of auto-scaling is also referred to as *concurrency-value-scaling* [22].

Remark 6. *Existing implementations of decentralized serverless architectures are asynchronous. In this setting, no dynamic performance model is available in the literature, to the best of our knowledge. The main motivation underlying this work has been to fill this gap.*

6 Conclusions

In cloud systems, load balancing and auto-scaling are key mechanisms to optimize both user-perceived delay performance and energy consumption. The focus of the existing literature has been on architectures where these mechanisms are synchronous or rely on a central queue. The novelty of our work is to consider an asynchronous and decentralized architecture. In the limit where the network demand grows in proportion to the nominal service capacity, our work provides a tractable framework to evaluate the impact of existing or new auto-scaling algorithms that are up to the platform user to choose or design. In addition, it provides a general condition under which, with a minimal communication overhead, it is possible to drive dynamics to the ideal situation where the user-perceived delay and the relative energy wastage induced by idle servers vanish. While this property also holds within the TABS scheme recently proposed in [26], our contribution consists in showing that it holds as well in asynchronous architectures provided that resources are scaled up if and only if the mean demand is greater than the rate at which servers become idle-on (Theorem 3). We have discussed in Remark 5 how such rate, $x_{0,1} + \beta x_{1,2}$, can be estimated over time but here one may employ other approaches, for instance based on machine learning techniques.

We discuss some perspectives and generalizations of our work:

- The load-balancing algorithms considered within our framework are Power-of- d and JBT- d . However, one may consider some of the algorithms mentioned in Section 5 as well to see, for example, whether fluid optimality can be obtained even without using JIQ (while keeping a comparable communication overhead).
- We have assumed that only one server at a time can be activated at each scaling time. Our framework and results generalize trivially to the case where a random number C of cold servers is selected instead of one, provided that the distribution of C does not depend on the overall number of servers N . Mutatis mutandis, it is enough to replace α by $\alpha \mathbb{E}[C]$.
- Blind- θ , see Definition 2, is the simplest scaling rule and it may be the best option in systems with a large number of dispatchers because in this setting the communication overhead induced by algorithms such as JIQ becomes a limiting factor. While Theorem 2 implies the existence of a unique fixed point, we leave as future work whether it is a global attractor. This is not trivial as one may check that natural adaptations of classical Lyapunov functions from queueing theory do not work.
- Since we have proposed a class, instead of a specific instance, of fluid optimal scaling rules, our work provides the system manager with some degrees of freedom when designing a suitable scale-up strategy. This opens the way to a new level of optimization problems such as the one presented in Section 4 as an application of our results.

References

- [1] Knative docs v1.3. <https://knative.dev/docs/>, 2022. Online; accessed: 2022-04-04.

- [2] Knative Load balancing. <https://knative.dev/docs/serving/load-balancing/>, 2022. Online; accessed: 2022-04-04.
- [3] Knative scale bounds. <https://knative.dev/docs/serving/autoscaling/scale-bounds/>, 2022. Online; accessed: 2022-04-04.
- [4] L. L. Andrew, M. Lin, and A. Wierman. Optimality, fairness, and robustness in speed scaling designs. In *Proceedings of the ACM SIGMETRICS International Conference on Measurement and Modeling of Computer Systems*, SIGMETRICS '10, page 37–48, New York, NY, USA, 2010. Association for Computing Machinery.
- [5] J. Anselmi. Combining size-based load balancing with round-robin for scalable low latency. *IEEE Transactions on Parallel and Distributed Systems*, 31(4):886–896, 2020.
- [6] J. Anselmi and F. Dufour. Power-of- d -choices with memory: Fluid limit and optimality. *Math. Oper. Res.*, 45(3):862–888, 2020.
- [7] R. Atar, I. Keslassy, G. Mendelson, A. Orda, and S. Vargaftik. Persistent-idle load-distribution. *Stochastic Systems*, 10(2):152–169, 2020.
- [8] M. Bramson. State space collapse with application to heavy traffic limits for multiclass queueing networks. *Queueing Syst. Theory Appl.*, 30(1/2):89–148, June 1998.
- [9] H. Chen and H.-Q. Ye. Asymptotic optimality of balanced routing. *Oper. Res.*, 60(1):163–179, Jan. 2012.
- [10] J. Dean and L. A. Barroso. The tail at scale. *Commun. ACM*, 56(2):74–80, Feb. 2013.
- [11] Y. Desmouceaux, M. Enguehard, and T. H. Clausen. Joint monitorless load-balancing and autoscaling for zero-wait-time in data centers. *IEEE Transactions on Network and Service Management*, 18(1):672–686, 2021.
- [12] Y. Desmouceaux, P. Pfister, J. Tollet, M. Townsley, and T. Clausen. Srlb: The power of choices in load balancing with segment routing. In *2017 IEEE 37th International Conference on Distributed Computing Systems (ICDCS)*, pages 2011–2016, 2017.
- [13] D. Gamarnik, J. N. Tsitsiklis, and M. Zubeldia. Delay, memory, and messaging tradeoffs in distributed service systems. In *Proceedings of the 2016 ACM SIGMETRICS International Conference on Measurement and Modeling of Computer Science*, SIGMETRICS '16, pages 1–12, New York, NY, USA, 2016. ACM.
- [14] D. Gamarnik, J. N. Tsitsiklis, and M. Zubeldia. Delay, memory, and messaging tradeoffs in distributed service systems. *Stochastic Systems*, 8(1):45–74, 2018.
- [15] A. Gandhi, S. Doroudi, M. Harchol-Balter, and A. Scheller-Wolf. Exact analysis of the m/m/k/setup class of markov chains via recursive renewal reward. In *Proceedings of the ACM SIGMETRICS/International Conference on Measurement and Modeling of Computer Systems*, SIGMETRICS '13, page 153–166, New York, NY, USA, 2013. Association for Computing Machinery.
- [16] D. Goldsztajn, A. Ferragut, F. Paganini, and M. Jonckheere. Controlling the number of active instances in a cloud environment. *SIGMETRICS Perform. Eval. Rev.*, 45(3):15–20, Mar. 2018.
- [17] V. Gupta and N. Walton. Load balancing in the nondegenerate slowdown regime. *Operations Research*, 67(1):281–294, 2019.
- [18] M. Harchol-Balter, M. E. Crovella, and C. D. Murta. On choosing a task assignment policy for a distributed server system. *Journal of Parallel and Distributed Computing*, 59(2):204 – 228, 1999.
- [19] M. Harchol-Balter, A. Scheller-Wolf, and A. R. Young. Surprising results on task assignment in server farms with high-variability workloads. SIGMETRICS '09, pages 287–298, New York, NY, USA, 2009. ACM.

- [20] Z. Liu and R. Righter. Optimal load balancing on distributed homogeneous unreliable processors. *Operations Research*, 46(4):563–573, 1998.
- [21] Y. Lu, Q. Xie, G. Kliot, A. Geller, J. R. Larus, and A. Greenberg. Join-idle-queue: A novel load balancing algorithm for dynamically scalable web services. *Perform. Eval.*, 68(11):1056–1071, Nov. 2011.
- [22] N. Mahmoudi and H. Khazaei. Performance modeling of serverless computing platforms. *IEEE Transactions on Cloud Computing*, pages 1–1, 2020.
- [23] N. Mahmoudi, C. Lin, H. Khazaei, and M. Litoiu. Optimizing serverless computing: Introducing an adaptive function placement algorithm. In *Proceedings of the 29th Annual International Conference on Computer Science and Software Engineering, CASCON '19*, page 203–213, USA, 2019. IBM Corp.
- [24] M. Mitzenmacher. The power of two choices in randomized load balancing. *IEEE Trans. Parallel Distrib. Syst.*, 12(10):1094–1104, Oct. 2001.
- [25] D. Mukherjee, S. C. Borst, J. S. H. van Leeuwen, and P. A. Whiting. Asymptotic Optimality of Power-of- d Load Balancing in Large-Scale Systems. *ArXiv e-prints*, Dec. 2016.
- [26] D. Mukherjee, S. Dhara, S. C. Borst, and J. S. van Leeuwen. Optimal service elasticity in large-scale distributed systems. *Proc. ACM Meas. Anal. Comput. Syst.*, 1(1), June 2017.
- [27] D. Mukherjee and A. Stolyar. Join idle queue with service elasticity: Large-scale asymptotics of a nonmonotone system. *Stochastic Systems*, 9(4):338–358, 2019.
- [28] H. Qian, D. Medhi, and K. Trivedi. A hierarchical model to evaluate quality of experience of online services hosted by cloud computing. In *12th IFIP/IEEE International Symposium on Integrated Network Management (IM 2011) and Workshops*, pages 105–112, 2011.
- [29] C. Qu, R. N. Calheiros, and R. Buyya. Auto-scaling web applications in clouds: A taxonomy and survey. *ACM Comput. Surv.*, 51(4), July 2018.
- [30] M. Shahrad, R. Fonseca, I. Goiri, G. Chaudhry, P. Batum, J. Cooke, E. Laureano, C. Tresness, M. Russinovich, and R. Bianchini. Serverless in the wild: Characterizing and optimizing the serverless workload at a large cloud provider. In *2020 USENIX Annual Technical Conference (USENIX ATC 20)*, pages 205–218. USENIX Association, July 2020.
- [31] U. Sharma, P. Shenoy, and D. F. Towsley. Provisioning multi-tier cloud applications using statistical bounds on sojourn time. In *Proceedings of the 9th International Conference on Autonomic Computing, ICAC '12*, page 43–52, New York, NY, USA, 2012. Association for Computing Machinery.
- [32] A. L. Stolyar. Pull-based load distribution in large-scale heterogeneous service systems. *Queueing Syst. Theory Appl.*, 80(4):341–361, Aug. 2015.
- [33] A. L. Stolyar. Pull-based load distribution among heterogeneous parallel servers: The case of multiple routers. *Queueing Syst. Theory Appl.*, 85(1-2):31–65, Feb. 2017.
- [34] J. N. Tsitsiklis and K. Xu. On the power of (even a little) resource pooling. *Stoch. Syst.*, 2(1):1–66, 2012.
- [35] M. van der Boor, S. Borst, and J. van Leeuwen. Load balancing in large-scale systems with multiple dispatchers. In *IEEE INFOCOM 2017 - IEEE Conference on Computer Communications*, pages 1–9, May 2017.
- [36] M. van der Boor, S. C. Borst, and J. van Leeuwen. Hyper-scalable JSQ with sparse feedback. *Proc. ACM Meas. Anal. Comput. Syst.*, 3(1):4:1–4:37, 2019.
- [37] M. van der Boor, S. C. Borst, J. S. van Leeuwen, and D. Mukherjee. Scalable load balancing in networked systems: A survey of recent advances. *arXiv preprint arXiv:1806.05444*, 2018.

- [38] E. van Eyk, A. Iosup, C. L. Abad, J. Grohmann, and S. Eismann. A spec rg cloud group’s vision on the performance challenges of faas cloud architectures. In *Companion of the 2018 ACM/SPEC International Conference on Performance Engineering, ICPE ’18*, page 21–24, New York, NY, USA, 2018. Association for Computing Machinery.
- [39] D. Villela, P. Pradhan, and D. Rubenstein. Provisioning servers in the application tier for e-commerce systems. In *Twelfth IEEE International Workshop on Quality of Service, 2004. IWQOS 2004.*, pages 57–66, 2004.
- [40] L. Wang, M. Li, Y. Zhang, T. Ristenpart, and M. Swift. Peeking behind the curtains of serverless platforms. In *Proceedings of the 2018 USENIX Conference on Usenix Annual Technical Conference, USENIX ATC ’18*, page 133–145, USA, 2018. USENIX Association.
- [41] L. Wang, M. Li, Y. Zhang, T. Ristenpart, and M. Swift. Peeking behind the curtains of serverless platforms. In *Proceedings of the 2018 USENIX Conference on Usenix Annual Technical Conference, USENIX ATC ’18*, page 133–145, USA, 2018. USENIX Association.
- [42] M. Weiser, B. Welch, A. Demers, and S. Shenker. Scheduling for reduced cpu energy. In *Proceedings of the 1st USENIX Conference on Operating Systems Design and Implementation, OSDI ’94*, page 2–es, USA, 1994. USENIX Association.
- [43] B. Yang, F. Tan, Y.-S. Dai, and S. Guo. Performance evaluation of cloud service considering fault recovery. In *Proceedings of the 1st International Conference on Cloud Computing, CloudCom ’09*, page 571–576, Berlin, Heidelberg, 2009. Springer-Verlag.

7 Proofs of Theorems 1, 2 and 3

We provide proofs for Theorems 1, 2 and 3.

7.1 Theorem 1: Connection between the Fluid and the Markov models

To prove Theorem 1, we follow two main steps. First, we use a common coupling technique to define the processes $(X^N(t))_{t \in [0, T]}$, for all $N \in \mathbb{Z}_+$, on a common probability space and show that limit trajectories exist and are Lipschitz continuous with probability one. The arguments used in this step are quite standard [34, 8, 13]. Then, we prove that limit trajectories are fluid solutions, which is the main technical difficulty, and here we develop arguments specific to our model.

7.1.1 Coupled Construction of Sample Paths

Let $\mathcal{N}_c(t)$ denote a Poisson process of rate c . We construct a probability space where the stochastic processes $\{(X^N(t))_{t \in [0, T]}\}_{N \geq 1}$ are coupled. All the processes of interest can be constructed in terms of the following mutually independent primitive processes:

- $\mathcal{N}_\phi(t)$, a Poisson process of rate $\phi := \lambda + 1 + \alpha + \beta + \gamma$. This process is defined on $(\Omega_E, \mathcal{A}_E, \mathbb{P}_E)$ and each jump of $\mathcal{N}_\phi(t)$ denotes the occurrence of an *event*.
- $(W_n)_n$, where the random variables W_n are $\{0, 1, 2, 3, 4\}$ -valued i.i.d. and such that $\mathbb{P}(W_n = 0) = \lambda/\phi$, $\mathbb{P}(W_n = 1) = 1/\phi$, $\mathbb{P}(W_n = 2) = \alpha/\phi$, $\mathbb{P}(W_n = 3) = \beta/\phi$ and $\mathbb{P}(W_n = 4) = \gamma/\phi$. This process is defined on $(\Omega_W, \mathcal{A}_W, \mathbb{P}_W)$ and will identify the *type* of the n -th event. Specifically, $W_n = 0$ indicates a job arrival, $W_n = 1$ a potential job departure, $W_n = 2$ a scaling time, $W_n = 3$ a potential server initialization, i.e., a server completed the initialization phase, and $W_n = 4$ a potential server expiration.
- $(A_n^p)_n$, $p = 1, \dots, d$, $(D_n)_n$, $(I_n)_n$, $(E_n)_n$ and $(R_n)_n$, where the random variables A_n^p , D_n , I_n , E_n and R_n , for all n , are all i.i.d. and uniform over the interval $[0, 1]$. The rvs A_n^p , D_n , I_n , E_n will be respectively used to select a server that i) will process an arriving job, ii) fires a departure, iii) fires an initialization and iv) fires an expiration. The rv R_n is related to the scaling rule and will decide whether a new server will be activated. These processes are defined on $(\Omega_S, \mathcal{A}_S, \mathbb{P}_S)$;

- $(X^N(0))_N$, the process of the initial conditions, where each random variable $X^N(0)$ takes values in \mathcal{S}_N . This process is defined on $(\Omega_0, \mathcal{A}_0, \mathbb{P}_0)$.

Using that $\mathcal{N}_\phi(Nt)$ and $\mathcal{N}_{\phi N}(t)$ are equal in distribution and the well-known fact that thinnings of a Poisson process produce independent Poisson processes, each process $\{(X^N(t))_{t \in [0, T]}\}$, $N \geq 1$, can be constructed on the product space, say $(\Omega, \mathcal{A}, \mathbb{P})$.

Now, let t_n be the time of the n -th jump of $\mathcal{N}_\phi(Nt)$. Let also $X^N(t^-) := \lim_{s \uparrow t} X^N(s)$, $Y_i^N(t) := \sum_{j=0}^i X_{j,2}^N(t)$ for all $i \geq 0$, $Y_{-1}^N(t) = 0$ and $\mathbf{1}_A^x = 1$ if $x \in A$ and 0 otherwise. The coordinates of $X^N(t)$ are then given by

$$X_{0,0}^N(t) = X_{0,0}^N(0) + \frac{1}{N} \sum_{n=1}^{\mathcal{N}_\phi(Nt)} \left(\mathbb{I}_{\{W_n=4\}} \mathbf{1}_{(0, X_{0,2}^N(t_n^-))}^{E_n} - \mathbb{I}_{\{W_n=2\}} \mathbb{I}_{\{X_{0,0}^N(t_n^-) > 0\}} \mathbf{1}_{(0, g(X^N(t_n^-)))}^{R_n} \right) \quad (22a)$$

$$X_{0,1}^N(t) = X_{0,1}^N(0) + \frac{1}{N} \sum_{n=1}^{\mathcal{N}_\phi(Nt)} \left(\mathbb{I}_{\{W_n=2\}} \mathbb{I}_{\{X_{0,0}^N(t_n^-) > 0\}} \mathbf{1}_{(0, g(X^N(t_n^-)))}^{R_n} - \mathbb{I}_{\{W_n=3\}} \mathbf{1}_{(0, X_{0,1}^N(t_n^-))}^{I_n} \right) \quad (22b)$$

$$X_{0,2}^N(t) = X_{0,2}^N(0) + \frac{1}{N} \sum_{n=1}^{\mathcal{N}_\phi(Nt)} \left(\mathbb{I}_{\{W_n=1\}} \mathbf{1}_{[Y_0^N(t_n^-), Y_1^N(t_n^-)]}^{D_n} - \mathbb{I}_{\{W_n=0\}} H_0(t_n^-) \right. \\ \left. + \mathbb{I}_{\{W_n=3\}} \mathbf{1}_{(0, X_{0,1}^N(t_n^-))}^{I_n} - \mathbb{I}_{\{W_n=4\}} \mathbf{1}_{(0, X_{0,2}^N(t_n^-))}^{E_n} \right) \quad (22c)$$

$$X_{i,2}^N(t) = X_{i,2}^N(0) + \frac{1}{N} \sum_{n=1}^{\mathcal{N}_\phi(Nt)} \left(\mathbb{I}_{\{W_n=0\}} (H_{i-1}(t_n^-) - H_i(t_n^-) \mathbb{I}_{\{i < B\}}) \right. \\ \left. + \mathbb{I}_{\{W_n=1\}} \left(\mathbf{1}_{(Y_{i-1}^N(t_n^-), Y_{i+1}^N(t_n^-))}^{D_n} - \mathbf{1}_{(Y_{i-1}^N(t_n^-), Y_i^N(t_n^-))}^{D_n} \right) \right) \quad (22d)$$

for all $i \geq 1$, where within Power-of- d (servers are selected with replacement)

$$H_i(t_n^-) := \prod_{p=1}^d \mathbf{1}_{(Y_{i-1}^N(t_n^-), 1]}^{A_p(1 - X_{0,0}^N(t_n^-) - X_{0,1}^N(t_n^-))} - \prod_{p=1}^d \mathbf{1}_{(Y_i^N(t_n^-), 1]}^{A_p(1 - X_{0,0}^N(t_n^-) - X_{0,1}^N(t_n^-))} \in \{0, 1\} \quad (23)$$

and within JBT- d

$$H_i(t_n^-) := \mathbf{1}_{(Y_{i-1}^N(t_n^-), Y_i^N(t_n^-))}^{A_n^1(1 - X_{0,0}^N(t_n^-) - X_{0,1}^N(t_n^-))} \mathbb{I}_{\{Y_d^N(t_n^-) = 0\}} + \mathbf{1}_{(Y_{i-1}^N(t_n^-), Y_i^N(t_n^-))}^{A_n^1 Y_d^N(t_n^-)} \mathbb{I}_{\{i \leq d\}} \mathbb{I}_{\{Y_d^N(t_n^-) > 0\}} \in \{0, 1\}. \quad (24)$$

These expressions follow by uniformization of $X^N(t)$. For instance, $X_{0,0}^N(t)$ has an upward jump of size $1/N$ at time t_n if the event occurring at that time is of type 4 (potential server expiration) and an idle-on server is actually selected at time t_n^- by the uniformized process. Analogously, $X_{0,0}^N(t)$ decreases by $1/N$ at time t_n if the event occurring at that time is of type 2, provided that at time t_n^- the cold servers pool is not empty and the scaling rule applies. Similar interpretations hold along the other coordinates of $X^N(t)$.

7.1.2 Tightness of Sample Paths and Lipschitz Property

We now prove tightness of sample paths. The lemmas in this section are equivalent to the lemmas in [14, Section 5.2].

Let us introduce the following formulas for quick reference.

Lemma 1. *Let $T > 0$. There exists $\mathcal{C} \subseteq \Omega$ such that $\mathbb{P}(\mathcal{C}) = 1$ and for all $\omega \in \mathcal{C}$:*

$$\lim_{N \rightarrow \infty} \sup_{t \in [0, T]} \left| \frac{1}{N} \mathcal{N}_\phi(Nt, \omega) - \phi t \right| = 0, \quad (25)$$

$$\lim_{N \rightarrow \infty} \sup_{t \in [0, T]} \left| \frac{1}{N} \sum_{n=1}^{\mathcal{N}_\phi(Nt, \omega)} \mathbb{I}_{\{W_n(\omega) = k\}} - \mathbb{P}(W_1 = k) \phi t \right| = 0, \quad k \in \{0, \dots, 4\} \quad (26)$$

$$\lim_{N \rightarrow \infty} \frac{1}{N} \sum_{n=1}^N \prod_{p=1}^d \mathbf{1}_{(a_p, b_p]^{c_p A_n^p}} = \prod_{p=1}^d \frac{b_p - a_p}{c_p}, \quad \forall a_p, b_p, c_p \in [0, 1], c_p > 0, p = 1, \dots, d. \quad (27)$$

Proof. This lemma directly follows by applying the functional strong law of large numbers for the Poisson process (for (25)), the fact that thinnings of a Poisson process produce independent Poisson processes (for (26)) and the strong law of the large numbers (for (27)). \square

We will work on a fixed ω that belongs to \mathcal{C} .

Let $x^0 \in [0, 1]$, sequences $A_N \downarrow 0$ and $B_N \downarrow 0$ be given. Let also $D[0, T]$ denote the Skorokhod space endowed with the uniform metric $d(x, y) := \sup_{t \in [0, T]} |x(t) - y(t)|$, for all $x, y \in D[0, T]$. For $N \geq 1$, let also

$$\begin{aligned} \mathcal{E}_N(B_N, A_N, x^0) &:= \{x \in D[0, T] : |x(0) - x^0| \leq B_N, |x(a) - x(b)| \leq \phi|a - b| + A_N, \forall a, b \in [0, T]\} \\ \mathcal{E}_c(x^0) &:= \{x \in D[0, T] : x(0) = x^0, |x(a) - x(b)| \leq \phi|a - b|, \forall a, b \in [0, T]\}. \end{aligned}$$

The next lemma says that the sample paths along any coordinate is approximately Lipschitz continuous. The proof is omitted because follows exactly the same standard arguments used in Lemma 5.2 of [14], which basically use the fact that the jumps of the Markov chain of interest are of the order of $1/N$ and that the evolution of such Markov chain on a given coordinate only depends on the evolution of such Markov chain on a finite number of other coordinates.

Lemma 2. *Fix $T > 0$, $\omega \in \mathcal{C}$, and some $x^0 \in \mathcal{S}_1$. Suppose that $\|X^N(\omega, 0) - x^0\|_w \leq \tilde{B}_N$, for some sequence $\tilde{B}_N \downarrow 0$. Then, there exists sequences $\{B_N^{(i,j)} \downarrow 0\}_{i,j}$ and $A_N \downarrow 0$ such that*

$$X_{i,j}^N(\omega, \cdot) \in \mathcal{E}_N(B_N^{(i,j)}, A_N, x^0), \quad \forall (i, j), \forall N. \quad (28)$$

The next proposition shows that any sequence of sample paths $X^N(\omega, t)$ contains a further subsequence that converges in $D^\infty[0, T]$, endowed with the metric $d^{\mathbb{Z}^+}(x, y) := \sup_{t \in [0, T]} \|x(t) - y(t)\|_w$, to a coordinate-wise Lipschitz continuous trajectory $x(t)$, as long as $\omega \in \mathcal{C}$. The proof is routine and omitted because it is a repetition of the argument used in the proof of Proposition 11 in [34] (equivalently, see also Proposition 5.3 in [14]).

Proposition 2. *Fix $T > 0$, $\omega \in \mathcal{C}$, and some $x^0 \in \mathcal{S}_1$. Suppose that $\|X^N(\omega, 0) - x^0\|_w \leq \tilde{B}_N$, for some sequence $\tilde{B}_N \downarrow 0$. Then, every subsequence of $\{X^N(\omega, \cdot)\}_{N=1}^\infty$ contains a further subsequence $\{X^{N_k}(\omega, \cdot)\}_{k=1}^\infty$ such that*

$$\lim_{k \rightarrow \infty} d^{\mathbb{Z}^+}(X^{N_k}, x) = 0 \quad (29)$$

where $x(0) = x^0$ and $x_{i,j} \in \mathcal{E}_c(x^0)$, for all i and j .

Since Lipschitz continuity implies absolute continuity, we have obtained that limit points of $X^N(t)$ exist and are absolutely continuous. Since all sample paths of $X^N(t)$ take values in \mathcal{S} , these limit points must belong as well to \mathcal{S} because \mathcal{S} is a closed set. Therefore, to conclude the proof of Theorem 1 it remains to show that the derivative of $x_{i,j}(t)$ is as in Definition 1 for all i and j , provided that t is a regular time. This is done in the next subsection and will also prove that a fluid solution started in $x^{(0)} \in \mathcal{S}_1$ exists.

7.1.3 Limit Trajectories are Fluid Solutions

Fix $\omega \in \mathcal{C}$ and let $\{X^{N_k}(\omega, t)\}_{k=1}^\infty$ be a subsequence that converges to \bar{x} (by Proposition 2), i.e.

$$\lim_{k \rightarrow \infty} \sup_{t \in [0, T]} \|X^{N_k}(\omega, t) - \bar{x}(t)\|_w = 0. \quad (30)$$

In the remainder, we fix such $\omega \in \mathcal{C}$ such that (30) holds and for simplicity we drop the dependency on ω . Since \bar{x} must be Lipschitz continuous (by Proposition 2), it is also absolutely continuous and to conclude the proof of Theorem 1, it remains to show that $\bar{x}(t)$ satisfies the conditions on the derivatives given in Definition 1 whenever $\bar{x}_{i,j}(t)$ is differentiable, for all i, j .

We say that t is a point of differentiability (of \bar{x}) if $x_{i,j}(t)$ is differentiable for all i, j .

We will (implicitly) use several times the following elementary lemma, which holds true because \bar{x} is a non-negative absolutely continuous function.

Lemma 3. *If $\bar{x}_{i,j}(t) = 0$ and t is a point of differentiability of $\bar{x}_{i,j}$, then $\dot{\bar{x}}_{i,j}(t) = 0$.*

Let $\epsilon > 0$. By Lemma 2, there exists a sequence $A_{N_k} \downarrow 0$ such that $X_{i,j}^{N_k}(\omega, u) \in [\bar{x}_{i,j}(t) - \epsilon\phi - A_{N_k}, \bar{x}_{i,j}(t) + \epsilon\phi + A_{N_k}]$, for all $u \in [t, t + \epsilon]$. Thus, for all k sufficiently large, $X_{i,j}^{N_k}(\omega, u) \in [\bar{x}_{i,j}(t) - 2\epsilon\phi, \bar{x}_{i,j}(t) + 2\epsilon\phi]$, for all $u \in [t, t + \epsilon]$. Thus, we have

$$|X_{i,j}^{N_k}(u) - \bar{x}_{i,j}(t)| \leq 2\phi\epsilon, \quad \forall u \in [t, t + \epsilon] \quad (31)$$

for all k sufficiently large. In addition, using (31) and that g is Lipschitz, we obtain

$$|g(X^{N_k}(u)) - g(\bar{x}(u))| \leq L \|X^{N_k}(u) - \bar{x}(u)\|_w \quad (32a)$$

$$\leq 2\phi\epsilon L \sqrt{\sum_{i,j} \frac{1}{2^{i+j}}} = 2\phi\epsilon L \sqrt{2}, \quad \forall u \in [t, t + \epsilon] \quad (32b)$$

where L is the Lipschitz constant of the scaling rule g .

We will refer to the following lemma, which is a straightforward consequence of (31) and of the strong law of the large numbers. In points where the fluid drift function is continuous, it will provide an expression for terms related to job departures, server initializations/departures and, in some cases, dispatching decisions.

Lemma 4. *Fix $\omega \in \mathcal{C}$ and let (30) hold. Then,*

$$\begin{aligned} \lim_{\epsilon \downarrow 0} \lim_{k \rightarrow \infty} \frac{1}{\epsilon N_k} \sum_{n=\mathcal{N}_\phi(N_k t)+1}^{\mathcal{N}_\phi(N_k(t+\epsilon))} \mathbb{I}_{\{W_n=1\}} \mathbf{1}_{(Y_{i-1}^n(t_n^-), Y_i^n(t_n^-))}^{D_n} &= \bar{x}_{i,2}(t) \\ \lim_{\epsilon \downarrow 0} \lim_{k \rightarrow \infty} \frac{1}{\epsilon N_k} \sum_{n=\mathcal{N}_\phi(N_k t)+1}^{\mathcal{N}_\phi(N_k(t+\epsilon))} \mathbb{I}_{\{W_n=3\}} \mathbf{1}_{(0, X_{0,1}^n(t_n^-))}^{I_n} &= \beta \bar{x}_{0,1}(t) \\ \lim_{\epsilon \downarrow 0} \lim_{k \rightarrow \infty} \frac{1}{\epsilon N_k} \sum_{n=\mathcal{N}_\phi(N_k t)+1}^{\mathcal{N}_\phi(N_k(t+\epsilon))} \mathbb{I}_{\{W_n=4\}} \mathbf{1}_{(0, X_{0,2}^n(t_n^-))}^{E_n} &= \gamma \bar{x}_{0,2}(t). \end{aligned}$$

In addition,

$$\lim_{\epsilon \downarrow 0} \lim_{k \rightarrow \infty} \frac{1}{\epsilon N_k} \sum_{n=\mathcal{N}_\phi(N_k t)+1}^{\mathcal{N}_\phi(N_k(t+\epsilon))} \mathbb{I}_{\{W_n=0\}} \mathbf{1}_{(Y_{i-1}^n(t_n^-), Y_i^n(t_n^-))}^{A_n^1 Y_d^N(t_n^-)} \mathbb{I}_{\{i \leq d\}} = \frac{\lambda \mathbb{I}_{\{i \leq d\}} \bar{x}_i(t)}{\sum_{j=0}^d \bar{x}_{j,2}(t)}$$

provided that $\sum_{j=0}^d \bar{x}_{j,2} > 0$, and

$$\lim_{\epsilon \downarrow 0} \lim_{k \rightarrow \infty} \frac{1}{\epsilon N_k} \sum_{n=\mathcal{N}_\phi(N_k t)+1}^{\mathcal{N}_\phi(N_k(t+\epsilon))} \mathbb{I}_{\{W_n=0\}} H_i(X^N(t_n^-)) = \lambda h_i(\bar{x})$$

provided that Power-of- d is used.

Proof. Given in Section 8. □

The next proposition proves the desired condition on the amount of fluid of cold and initializing servers.

Proposition 3. *Fix $\omega \in \mathcal{C}$, let (30) hold and assume that t is a point of differentiability. Then,*

$$\dot{\bar{x}}_{0,0} = \gamma \bar{x}_{0,2}(t) - \alpha \mathbb{I}_{\{\bar{x}_{0,0}(t) > 0\}} g(\bar{x}(t)) - \gamma \bar{x}_{0,2}(t) \mathbb{I}_{\{\bar{x}_{0,0}(t) = 0, \gamma \bar{x}_{0,2}(t) \leq \alpha g(\bar{x}(t))\}} \quad (33)$$

$$\dot{\bar{x}}_{0,1} = \alpha g(\bar{x}(t)) \mathbb{I}_{\{\bar{x}_{0,0}(t) > 0\}} - \beta \bar{x}_{0,1}(t) + \gamma \bar{x}_{0,2}(t) \mathbb{I}_{\{\bar{x}_{0,0}(t) = 0, \gamma \bar{x}_{0,2}(t) \leq \alpha g(\bar{x}(t))\}}. \quad (34)$$

Proof. Assume that $\bar{x}_{0,0}(t) > 0$ and let $\epsilon \in (0, \frac{\bar{x}_{0,0}(t)}{2\phi})$. Given that

$$t_n \in (t, t + \epsilon] \text{ whenever } n \in \{\mathcal{N}_\phi(N_k t) + 1, \dots, \mathcal{N}_\phi(N_k(t + \epsilon))\}, \quad (35)$$

(31) implies that for all k sufficiently large, $|X_{0,0}^{N_k}(t_n^-) - \bar{x}_{0,0}(t)| \leq 2\phi\epsilon < \bar{x}_{0,0}(t)$ and thus $X_{0,0}^{N_k}(t_n^-) > 0$. We have shown that

$$\mathbb{I}_{\{X_{0,0}^{N_k}(t_n^-) > 0\}} = 1, \quad \forall n \in \{\mathcal{N}_\phi(N_k t) + 1, \dots, \mathcal{N}_\phi(N_k(t + \epsilon))\} \quad (36)$$

for all k sufficiently large. Using (22), Lemma 4 and (36), we have

$$\begin{aligned} \dot{\bar{x}}_{0,0}(t) &= \lim_{\epsilon \downarrow 0} \frac{1}{\epsilon} \lim_{k \rightarrow \infty} \left(X_{0,0}^{N_k}(t + \epsilon) - X_{0,0}^{N_k}(t) \right) \\ &= \lim_{\epsilon \downarrow 0} \lim_{k \rightarrow \infty} \frac{1}{\epsilon N_k} \sum_{n=\mathcal{N}_\phi(N_k t)+1}^{\mathcal{N}_\phi(N_k(t+\epsilon))} \left(\mathbb{I}_{\{W_n=4\}} \mathbf{1}_{(0, X_{0,0}^{N_k}(t_n^-))}^{E_n} - \mathbb{I}_{\{W_n=2\}} \mathbb{I}_{\{X_{0,0}^{N_k}(t_n^-) > 0\}} \mathbf{1}_{(0, g(X^{N_k}(t_n^-)))}^{R_n} \right) \end{aligned} \quad (37a)$$

$$= \gamma \bar{x}_{0,2}(t) - \lim_{\epsilon \downarrow 0} \lim_{k \rightarrow \infty} \frac{1}{\epsilon N_k} \sum_{n=\mathcal{N}_\phi(N_k t)+1}^{\mathcal{N}_\phi(N_k(t+\epsilon))} \mathbb{I}_{\{W_n=2\}} \mathbf{1}_{(0, g(X^{N_k}(t_n^-)))}^{R_n}. \quad (37b)$$

Since t is a point of differentiability, the double limit in the RHS of (37b) exists. Then, (32) implies that given $\epsilon > 0$ small enough, $g(X^{N_k}(t_n^-)) \in [g(\bar{x}(t)) - 2\phi\epsilon L\sqrt{2}, g(\bar{x}(t)) + 2\phi\epsilon L\sqrt{2}]$ for all k sufficiently large. Combining these bounds with Lemma 1 and letting $\epsilon \downarrow 0$ (as in the proof of Lemma 4), we obtain

$$\lim_{\epsilon \downarrow 0} \lim_{k \rightarrow \infty} \frac{1}{\epsilon N_k} \sum_{n=\mathcal{N}_\phi(N_k t)+1}^{\mathcal{N}_\phi(N_k(t+\epsilon))} \mathbb{I}_{\{W_n=2\}} \mathbf{1}_{(0, g(X^{N_k}(t_n^-)))}^{R_n} = \alpha g(\bar{x}(t)). \quad (38)$$

Similarly, on coordinates (0,1), we obtain

$$\begin{aligned} \dot{\bar{x}}_{0,1}(t) &= \lim_{\epsilon \downarrow 0} \frac{1}{\epsilon} \lim_{k \rightarrow \infty} \left(X_{0,1}^{N_k}(t + \epsilon) - X_{0,1}^{N_k}(t) \right) \\ &= \lim_{\epsilon \downarrow 0} \lim_{k \rightarrow \infty} \frac{1}{\epsilon N_k} \sum_{n=\mathcal{N}_\phi(N_k t)+1}^{\mathcal{N}_\phi(N_k(t+\epsilon))} \left(\mathbb{I}_{\{W_n=2\}} \mathbb{I}_{\{X_{0,0}^{N_k}(t_n^-) > 0\}} \mathbf{1}_{(0, g(X^{N_k}(t_n^-)))}^{R_n} - \mathbb{I}_{\{W_n=3\}} \mathbf{1}_{(0, X_{0,1}^{N_k}(t_n^-))}^{I_n} \right) \\ &= \alpha g(\bar{x}) - \beta \bar{x}_{0,1}(t). \end{aligned}$$

Now, let us assume that $\bar{x}_{0,0}(t) = 0$. First, we notice that

$$\begin{aligned} \dot{\bar{x}}_{0,0}(t) &= \gamma \bar{x}_{0,2}(t) - \lim_{\epsilon \downarrow 0} \lim_{k \rightarrow \infty} \frac{1}{\epsilon N_k} \sum_{n=\mathcal{N}_\phi(N_k t)+1}^{\mathcal{N}_\phi(N_k(t+\epsilon))} \mathbb{I}_{\{W_n=2\}} \mathbb{I}_{\{X_{0,0}^{N_k}(t_n^-) > 0\}} \mathbf{1}_{(0, g(X^{N_k}(t_n^-)))}^{R_n} \\ &\geq \gamma \bar{x}_{0,2}(t) - \lim_{\epsilon \downarrow 0} \lim_{k \rightarrow \infty} \frac{1}{\epsilon N_k} \sum_{n=\mathcal{N}_\phi(N_k t)+1}^{\mathcal{N}_\phi(N_k(t+\epsilon))} \mathbb{I}_{\{W_n=2\}} \mathbf{1}_{(0, g(X^{N_k}(t_n^-)))}^{R_n} = \gamma \bar{x}_{0,2}(t) - \alpha g(\bar{x}) \end{aligned} \quad (39)$$

where the first equality follows by (37a) and Lemma 4, and the last equality follows by (38). Thus, if $\bar{x}_{0,0}(t) = 0$ and $\gamma \bar{x}_{0,2}(t) > \alpha g(\bar{x})$, then by the previous inequality $\dot{\bar{x}}_{0,0}(t) > 0$, which is not possible because if t is a point of differentiability and $\bar{x}_{0,0}(t) = 0$ then necessarily $\dot{\bar{x}}_{0,0}(t) = 0$ as $\bar{x}_{0,0}$ is a non-negative absolutely continuous function. Thus, in a point of differentiability t where $\bar{x}_{0,0}(t) = 0$, we must have $\gamma \bar{x}_{0,2}(t) \leq \alpha g(\bar{x})$. and, necessarily, $\dot{\bar{x}}_{0,0}(t) = 0$. In this case, (39) gives

$$\gamma \bar{x}_{0,2}(t) = \lim_{k \rightarrow \infty} \frac{1}{\epsilon N_k} \sum_{n=\mathcal{N}_\phi(N_k t)+1}^{\mathcal{N}_\phi(N_k(t+\epsilon))} \mathbb{I}_{\{W_n=2\}} \mathbb{I}_{\{X_{0,0}^{N_k}(t_n^-) > 0\}} \mathbf{1}_{(0, g(X^{N_k}(t_n^-)))}^{R_n}. \quad (40)$$

This term is interpreted as the amount of idle-on servers that become cold but instantly turn initializing. Substituting (40) in the previous equalities within the conditions $\gamma \bar{x}_{0,2}(t) \leq \alpha g(\bar{x})$ and $\bar{x}_{0,0}(t) = 0$, we obtain (33) and (34). \square

On the coordinates associated to warm servers, it remains to prove that

$$\dot{\bar{x}}_{0,2}(t) = \bar{x}_{1,2}(t) - \lambda h_0(\bar{x}(t)) + \beta \bar{x}_{0,1}(t) - \gamma \bar{x}_{0,2}(t) \quad (41)$$

$$\dot{\bar{x}}_{i,2}(t) = \bar{x}_{i+1,2}(t) \mathbb{I}_{\{i < B\}} - \bar{x}_{i,2}(t) + \lambda (h_{i-1}(\bar{x}(t)) - h_i(\bar{x}(t)) \mathbb{I}_{\{i < B\}}), \quad i \geq 1, \quad (42)$$

whenever t is a point of differentiability of \bar{x} . Let

$$\mathcal{H}_i(t) := \lim_{\epsilon \downarrow 0} \lim_{k \rightarrow \infty} \frac{1}{\epsilon N_k} \sum_{n=\mathcal{N}_\phi(N_k t)+1}^{\mathcal{N}_\phi(N_k(t+\epsilon))} \mathbb{I}_{\{W_n=0\}} H_i(t_n^-) \geq 0, \quad (43)$$

which is interpreted as the rate at which jobs are assigned to warm servers with exactly i jobs. Using Lemma 4 and (22), we have

$$\dot{\bar{x}}_{0,2}(t) = \lim_{\epsilon \downarrow 0} \frac{1}{\epsilon} \lim_{k \rightarrow \infty} \left(X_{0,2}^{N_k}(t+\epsilon) - X_{0,2}^{N_k}(t) \right) = \bar{x}_{1,2}(t) - \mathcal{H}_0(t) + \beta \bar{x}_{0,1}(t) - \gamma \bar{x}_{0,2}(t) \quad (44a)$$

$$\dot{\bar{x}}_{i,2}(t) = \lim_{\epsilon \downarrow 0} \frac{1}{\epsilon} \lim_{k \rightarrow \infty} \left(X_{i,2}^{N_k}(t+\epsilon) - X_{i,2}^{N_k}(t) \right) = \bar{x}_{i+1,2}(t) \mathbb{I}_{\{i < B\}} - \bar{x}_{i,2}(t) + \mathcal{H}_{i-1}(t) - \mathcal{H}_i(t) \mathbb{I}_{\{i < B\}}. \quad (44b)$$

In the following, we need to show that $\mathcal{H}_i(t) = h_i(\bar{x}(t))$ where the h_i 's are as in Definition 1. We treat the cases of Power-of- d and JBT- d separately.

Lemma 5. *Assume that Power-of- d is applied. Then, (41) and (42) hold true.*

Proof. If $\bar{x}_{0,0} + \bar{x}_{0,1} < 1$, then the structure of the H_i 's in (23) and Lemma 4 immediately give (41) and (42). Now, let us assume that $\bar{x}_{0,0} + \bar{x}_{0,1} = 1$. On coordinate (0,2), in a point of differentiability we necessarily have $\dot{\bar{x}}_{0,2} = 0$. Using Lemma 4 and (22), we obtain

$$\dot{\bar{x}}_{0,2}(t) = \lim_{\epsilon \downarrow 0} \frac{1}{\epsilon} \lim_{k \rightarrow \infty} \left(X_{0,2}^{N_k}(t+\epsilon) - X_{0,2}^{N_k}(t) \right) = \beta \bar{x}_{0,1}(t) - \mathcal{H}_0(t) = 0. \quad (45)$$

Similarly, on coordinate (1,2), Lemma 4 and (45) imply that in a point of differentiability we have $\dot{\bar{x}}_{1,2}(t) = \mathcal{H}_0(t) - \mathcal{H}_1(t) = 0$ and thus $\mathcal{H}_1(t) = \mathcal{H}_0(t) = \beta \bar{x}_{0,1}(t)$. Then, on coordinate $(i, 2)$ by induction we obtain $\mathcal{H}_i(t) = \mathcal{H}_{i-1}(t) = \beta \bar{x}_{0,1}(t)$. On the other hand, we also have

$$\dot{\bar{x}}_{0,2}(t) = \beta \bar{x}_{0,1}(t) - \lim_{\epsilon \downarrow 0} \frac{1}{\epsilon} \lim_{k \rightarrow \infty} \frac{1}{\epsilon N_k} \sum_{n=\mathcal{N}_\phi(N_k t)+1}^{\mathcal{N}_\phi(N_k(t+\epsilon))} \mathbb{I}_{\{W_n=0\}} H_0(t_n^-) \geq \beta \bar{x}_{0,1}(t) - \lambda \quad (46)$$

where in the last inequality we have just used that $H_0(t_n^-) \leq 1$. Thus, if $\beta \bar{x}_{0,1}(t) > \lambda$, we get a contradiction and t can not be a point of differentiability. Substituting $\mathcal{H}_i(t) = \beta \bar{x}_{0,1}(t)$ in (44) when $\beta \bar{x}_{0,1}(t) \leq \lambda$, we obtain (41) and (42). \square

The case of JBT- d is more delicate than Power-of- d because of the discontinuous structure of the H_i 's when $\sum_{j=0}^d X_{j,2}^N(t_n^-) = 0$, see (24). In addition to a more involved argument than the one presented in the proof of Lemma 5, which we will develop in Lemma 7 below, we need the following lemma, which we will use to determine an expression for \mathcal{H}_i when $\sum_{j=0}^d \bar{x}_{j,2}(t) = 0$.

Lemma 6. *Assume that $\bar{x}(t)$ satisfies $\bar{x}_{0,0}(t) + \bar{x}_{0,1}(t) < 1$. Then, for all i*

$$\begin{aligned} & \lim_{\epsilon \downarrow 0} \lim_{k \rightarrow \infty} \frac{1}{\epsilon N_k} \sum_{n=\mathcal{N}_\phi(N_k t)+1}^{\mathcal{N}_\phi(N_k(t+\epsilon))} \mathbb{I}_{\{W_n=0\}} \mathbf{1}_{\left(\frac{A_n^1(1-X_{0,0}^{N_k}(t_n^-) - X_{0,1}^{N_k}(t_n^-))}{(Y_{i-1}^{N_k}(t_n^-), Y_i^{N_k}(t_n^-))} \right)} \mathbb{I}_{\{\sum_{j=0}^d X_{j,2}^{N_k}(t_n^-) > 0\}} \\ &= \frac{\bar{x}_{i,2}(t)}{1 - \bar{x}_{0,0}(t) - \bar{x}_{0,1}(t)} \lim_{\epsilon \downarrow 0} \lim_{k \rightarrow \infty} \frac{1}{\epsilon N_k} \sum_{n=\mathcal{N}_\phi(N_k t)+1}^{\mathcal{N}_\phi(N_k(t+\epsilon))} \mathbb{I}_{\{W_n=0\}} \mathbb{I}_{\{\sum_{j=0}^d X_{j,2}^{N_k}(t_n^-) > 0\}}. \quad (47) \end{aligned}$$

Proof. Given in Section 8. \square

The following lemma proves the desired property in the case of JBT- d .

Lemma 7. *Assume that JBT- d is applied. Then, (41) and (42) hold true.*

Proof. We analyze \mathcal{H}_i and the resulting expression will be substituted in (44). This will give (41) and (42).

First, if $\bar{x}_{0,0} + \bar{x}_{0,1} = 1$, the argument in the proof of Lemma 5 gives i) $\mathcal{H}_i(t) = \beta\bar{x}_{0,1}(t)$ when $\beta\bar{x}_{0,1}(t) \leq \lambda$ and ii) t not a point of differentiability when $\beta\bar{x}_{0,1}(t) > \lambda$. This gives (41) and (42) (when $\bar{x}_{0,0} + \bar{x}_{0,1} = 1$) and in the remainder we assume that $\bar{x}_{0,0} + \bar{x}_{0,1} < 1$.

Let us now assume that $\sum_{j=0}^d \bar{x}_{j,2}(t) > 0$ and let $\epsilon \in (0, \frac{\sum_{j=0}^d \bar{x}_{j,2}(t)}{2\phi(d+1)})$. Since $t_n \in (t, t + \epsilon]$ whenever $n \in \{\mathcal{N}_\phi(N_k t) + 1, \dots, \mathcal{N}_\phi(N_k(t + \epsilon))\}$, (31) and the triangular inequality imply that for all k sufficiently large $|\sum_{j=0}^d X_{j,2}^{N_k}(t_n) - \bar{x}_{j,2}(t)| \leq 2(d+1)\phi\epsilon < \sum_{j=0}^d \bar{x}_{j,2}(t)$ and thus $\sum_{j=0}^d X_{j,2}^{N_k}(t_n) > 0$. We have shown that

$$\mathbb{I}_{\{\sum_{j=0}^d X_{j,2}^{N_k}(t_n) > 0\}} = 1, \quad \forall n \in \{\mathcal{N}_\phi(N_k t) + 1, \dots, \mathcal{N}_\phi(N_k(t + \epsilon))\} \quad (48)$$

for all k sufficiently large, given $\epsilon > 0$ sufficiently small. Substituting (48) in (24) and applying Lemma 4, we obtain (41) and (42) (under the conditions $\bar{x}_{0,0} + \bar{x}_{0,1} < 1$ and $\sum_{j=0}^d \bar{x}_{j,2}(t) > 0$).

It remains to understand the terms \mathcal{H}_i in the case where $\sum_{j=0}^d \bar{x}_{j,2}(t) = 0$, which we assume in the remainder of the proof.

Suppose that t is a point of differentiability. Then, by applying Lemma 4 to $X_{0,2}^N$ (see (22)), we obtain

$$\dot{\bar{x}}_{0,2}(t) = \lim_{\epsilon \downarrow 0} \frac{1}{\epsilon} \lim_{k \rightarrow \infty} X_{0,2}^{N_k}(t + \epsilon) - X_{0,2}^{N_k}(t) = \bar{x}_{1,2}(t)\mathbb{I}_{\{d=0\}} + \beta\bar{x}_{0,1}(t) - \mathcal{H}_0(t), \quad (49)$$

and given that necessarily $\dot{\bar{x}}_{0,2}(t) = 0$, we obtain

$$\mathcal{H}_0(t) = \bar{x}_{1,2}(t)\mathbb{I}_{\{d=0\}} + \beta\bar{x}_{0,1}(t). \quad (50)$$

Similarly, on coordinate $(i, 2)$, with $0 < i \leq d$, we obtain

$$\dot{\bar{x}}_{i,2}(t) = \bar{x}_{i+1,2}(t)\mathbb{I}_{\{i=d\}} + \mathcal{H}_{i-1}(t) - \mathcal{H}_i(t) = 0. \quad (51)$$

By induction, this gives $\mathcal{H}_i(t) = \mathcal{H}_0(t) = \beta\bar{x}_{0,1}(t)$ for all $i < d$ and $\mathcal{H}_d(t) = \beta\bar{x}_{0,1}(t) + \bar{x}_{d+1,2}(t)$, that is,

$$\mathcal{H}_i(t) = \beta\bar{x}_{0,1}(t) + \bar{x}_{d+1,2}(t)\mathbb{I}_{\{i=d\}}, \quad i \leq d. \quad (52)$$

We have proven (52) under the hypothesis that t was a point of differentiability but now we show that $\bar{x}(t)$ is not differentiable if $\lambda < \bar{x}_{d+1,2} + (d+1)\beta\bar{x}_{0,1}$. Towards this purpose, first we notice that

$$\begin{aligned} \sum_{i=0}^d \mathcal{H}_i(t) &= \lim_{\epsilon \downarrow 0} \lim_{k \rightarrow \infty} \frac{1}{\epsilon N_k} \sum_{n=\mathcal{N}_\phi(N_k t)+1}^{\mathcal{N}_\phi(N_k(t+\epsilon))} \mathbb{I}_{\{W_n=0\}} \sum_{i=0}^d H_i(t_n^-) \\ &= \lim_{\epsilon \downarrow 0} \lim_{k \rightarrow \infty} \frac{1}{\epsilon N_k} \sum_{n=\mathcal{N}_\phi(N_k t)+1}^{\mathcal{N}_\phi(N_k(t+\epsilon))} \mathbb{I}_{\{W_n=0\}} \mathbb{I}_{\{\sum_{j=0}^d X_{j,2}^N(t_n^-) > 0\}} \leq \lim_{\epsilon \downarrow 0} \lim_{k \rightarrow \infty} \frac{1}{\epsilon N_k} \sum_{n=\mathcal{N}_\phi(N_k t)+1}^{\mathcal{N}_\phi(N_k(t+\epsilon))} \mathbb{I}_{\{W_n=0\}} = \lambda. \end{aligned}$$

Here, the first equality follows because the limits $\mathcal{H}_i(t)$ exist and the second inequality follows by the fact that (recall the definition of \mathcal{H}_i in (43))

$$\sum_{i=0}^d H_i(t_n^-) = \mathbb{I}_{\{\sum_{j=0}^d X_{j,2}^N(t_n^-) > 0\}} + \mathbf{1}_{(0, Y_d^N(t_n^-))}^{A_n^1(1 - X_{0,0}^N(t_n^-) - X_{0,1}^N(t_n^-))} \mathbb{I}_{\{\sum_{j=0}^d X_{j,2}^N(t_n^-) = 0\}} \quad (53)$$

and by Lemma 4 because $\sum_{j=0}^d \bar{x}_{j,2}(t) = 0$. Then, using (52), we necessarily have

$$\sum_{i=0}^d \mathcal{H}_i(t) = \bar{x}_{d+1,2}(t) + (d+1)\beta\bar{x}_{0,1}(t) \leq \lambda \quad (54)$$

and, given that necessarily $\mathcal{H}_i \geq 0$, we conclude that t can not be a point of differentiability whenever (54) does not hold true.

Now, we investigate \mathcal{H}_i when $i > d$ and assuming that (54) holds as otherwise $\bar{x}(t)$ would not be differentiable. We have

$$\begin{aligned}
\mathcal{H}_i(t) &= \frac{\lambda \bar{x}_{i,2}(t)}{1 - \bar{x}_{0,0}(t) - \bar{x}_{0,1}(t)} - \lim_{\epsilon \downarrow 0} \lim_{k \rightarrow \infty} \frac{1}{\epsilon N_k} \sum_{n=\mathcal{N}_\phi(N_k t)+1}^{\mathcal{N}_\phi(N_k(t+\epsilon))} \mathbb{I}_{\{W_n=0\}} \mathbf{1}_{(Y_{i-1}^N(t_n^-), Y_i^N(t_n^-)]} A_n^1(1-X_{0,0}^N(t_n^-)-X_{0,1}^N(t_n^-)) \mathbb{I}_{\{\sum_{j=0}^d X_{j,2}^N(t_n^-) > 0\}} \\
&= \frac{\lambda \bar{x}_{i,2}(t)}{1 - \bar{x}_{0,0}(t) - \bar{x}_{0,1}(t)} - \frac{\bar{x}_{i,2}(t)}{1 - \bar{x}_{0,0}(t) - \bar{x}_{0,1}(t)} \lim_{\epsilon \downarrow 0} \lim_{k \rightarrow \infty} \frac{1}{\epsilon N_k} \sum_{n=\mathcal{N}_\phi(N_k t)+1}^{\mathcal{N}_\phi(N_k(t+\epsilon))} \mathbb{I}_{\{W_n=0\}} \mathbb{I}_{\{\sum_{j=0}^d X_{j,2}^N(t_n^-) > 0\}} \\
&= \frac{\lambda \bar{x}_{i,2}(t)}{1 - \bar{x}_{0,0}(t) - \bar{x}_{0,1}(t)} - \frac{\bar{x}_{i,2}(t)}{1 - \bar{x}_{0,0}(t) - \bar{x}_{0,1}(t)} \sum_{i=0}^d \mathcal{H}_i(t) \\
&= \bar{x}_{i,2}(t) \frac{\lambda - \bar{x}_{d+1,2}(t) - (d+1)\beta \bar{x}_{0,1}(t)}{1 - \bar{x}_{0,0}(t) - \bar{x}_{0,1}(t)}.
\end{aligned}$$

In the first equality, we have used (24) and applied Lemma 4 to the definition of \mathcal{H}_i in (43); In the second, we have applied Lemma 6. In the third, we have used (53) and that

$$0 \leq \lim_{\epsilon \downarrow 0} \lim_{k \rightarrow \infty} \frac{1}{\epsilon N_k} \mathbf{1}_{(0, Y_d^N(t_n^-)]} A_n^1(1-X_{0,0}^N(t_n^-)-X_{0,1}^N(t_n^-)) \mathbb{I}_{\{\sum_{j=0}^d X_{j,2}^N(t_n^-) = 0\}} \leq \lim_{\epsilon \downarrow 0} \lim_{k \rightarrow \infty} \frac{1}{\epsilon N_k} \mathbf{1}_{(0, Y_d^N(t_n^-)]} A_n^1(1-X_{0,0}^N(t_n^-)-X_{0,1}^N(t_n^-)) = 0$$

with the last inequality following by Lemma 4 as $\sum_{j=0}^d \bar{x}_{j,2}(t) = 0$; in the fourth, we have substituted (52). This concludes the proof. \square

Thus, we have shown that \bar{x} is a fluid solution.

7.2 Proof of Theorem 2: Fixed points

We now prove Theorem 2. By definition, $x \in \mathcal{S}_1$ is a fixed point if and only if

$$0 = \gamma x_{0,2} - \alpha g \mathbb{I}_{\{x_{0,0} > 0\}} - \gamma x_{0,2} \mathbb{I}_{\{x_{0,0}=0, \gamma x_{0,2} \leq \alpha g\}} \quad (55a)$$

$$0 = \alpha g \mathbb{I}_{\{x_{0,0} > 0\}} - \beta x_{0,1} + \gamma x_{0,2} \mathbb{I}_{\{x_{0,0}=0, \gamma x_{0,2} \leq \alpha g\}} \quad (55b)$$

$$0 = x_{1,2} - h_0(x) + \beta x_{0,1} - \gamma x_{0,2} \quad (55c)$$

$$0 = x_{i+1,2} - x_{i,2} + h_{i-1}(x) - h_i(x), \quad i \geq 1. \quad (55d)$$

Together with $\|x\| = 1$, we now show that these conditions coincide with (8).

If i) $x_{0,0} = 0$ and $\gamma x_{0,2} > \alpha g$, or if ii) $x_{0,0} + x_{0,1} = 1$, then we easily observe that x cannot be a fixed point. Therefore, in the following we exclude these conditions. Now, summing (55a) and (55b), we obtain

$$\beta x_{0,1} = \gamma x_{0,2} \quad (56)$$

which gives (8b). Then, (8c) and (8d) directly follow from (55a) and (55b).

Substituting (56) in (55c), the conditions (55c)-(55d) become

$$0 = x_{1,2} - h_0(x) \quad (57a)$$

$$0 = x_{i+1,2} - x_{i,2} + h_{i-1}(x) - h_i(x), \quad i \geq 1, \quad (57b)$$

and taking summations

$$x_{i,2} = h_{i-1}(x), \quad i \geq 1. \quad (58)$$

The equations in (57) are interpreted as the mean-field fixed-point equations associated to Power-of- d and JBT- d when the number of servers is Ny_0 instead of N ; we recall that $y_i = \sum_{i \geq 0} x_{i,2}$ is the proportion of warm servers with at least i jobs. Within Power-of- d , one can directly check that for any given $x_{0,2}$, (58) holds if and only if $x_{i,2}$ is given by (8e) and that, after a substitution, this gives $\sum_{i \geq 1} x_{i,2} = \lambda$ so that (8a) must hold true. The following lemma, given in Section 8, handles the more delicate case of JBT- d .

Lemma 8. *Within JBT-d, for any given $x_{0,2}$, (57) holds if and only if $x_{i,2}$ satisfies (8f)-(8j). In addition, (8a) holds true.*

Therefore, the conditions in (55) are equivalent to (8). This proves the first statement of Theorem 2.

Now, under Assumption 3, $x_{i,2}$ is a function of $x_{0,2}$, for all $i \geq 1$, and we write $x_{i,2}$ as a shorthand notation for $x_{i,2}(x_{0,2})$. Using (56), we can then focus only on the following conditions:

$$x_{0,0} + \left(\frac{\gamma}{\beta} + 1\right)x_{0,2} = 1 - \lambda \quad (59a)$$

$$\gamma x_{0,2} \leq \alpha g, \quad \text{if } x_{0,0} = 0 \quad (59b)$$

$$\gamma x_{0,2} = \alpha g, \quad \text{if } x_{0,0} > 0. \quad (59c)$$

Here, we notice that $(x_{0,0}^\circ, x_{0,2}^\circ) = (0, \frac{\beta}{\beta+\gamma}(1-\lambda))$ uniquely solves (59) if

$$\left(\frac{1}{\beta} + \frac{1}{\gamma}\right)\alpha g(x^\circ) \geq 1 - \lambda \quad (60)$$

where x° is uniquely determined by $(x_{0,0}^\circ, x_{0,2}^\circ)$. So, let us assume that (60) does *not* hold true. Then, if a point $(x_{0,0}, x_{0,2}) \in [0, 1]^2$ that solves (59) exists, then necessarily $x_{0,0} > 0$ as otherwise $x_{0,2} = x_{0,2}^\circ$ (by (59a)) and (60) would hold, contradicting the hypothesis. This proves the second part of Theorem 2.

7.3 Proof of Theorem 3: Fluid Optimality

We give a proof for Theorem 3. The non-linear structure taken by the h_i 's when $x_{0,2} = 0$, see (7), complicates the analysis and the identification of a Lyapunov function. For this reason, our strategy is based on a divide-and-conquer approach. This will actually provide insights about the dynamics followed by fluid solutions. For simplicity, we provide a proof assuming that $B < \infty$, which is essentially equivalent to assume that $x_{i,2}(0) = 0$ for all i large enough; this is not critical as $x_{i,2}^* = 0$ for all $i \geq 2$.

Let $\bar{Q}(x) := \sum_{i=1}^B ix_{i,2}$, i.e., the overall number of jobs in the system in state x . The following lemma gives a property on the time derivative of $\bar{Q}(x(t))$.

Lemma 9. *Let $x(t)$ be a fluid solution induced by JIQ such that $x(0) \in \mathcal{S}_1$ and $B < \infty$. If t is a point of differentiability, then*

$$\dot{\bar{Q}}(x(t)) = \lambda - y_1(t). \quad (61)$$

Proof. First, we notice that

$$\dot{\bar{Q}}(x(t)) = \sum_{i \geq 1} i \dot{x}_{i,2}(t) = -y_1 + \sum_{i=0}^{B-1} h_i(x(t)) \quad (62)$$

where the second equality follows by applying Definition 1. Now, we treat the cases $x_{0,2}(t) > 0$ and $x_{0,2}(t) = 0$ separately. Suppose that $x_{0,2}(t) > 0$. Then, $h_i(x(t)) = \lambda \mathbb{1}_{\{i=0\}}$ (by (7)) and substituting in (62) we immediately get $\dot{\bar{Q}}(x(t)) = \lambda - y_1(t)$ as desired. Thus, suppose in the remainder that $x_{0,2}(t) = 0$. Now, assume that $y_0(t) > 0$. Then, using again (7),

$$\begin{aligned} \dot{\bar{Q}}(x(t)) &= -y_1 + (\beta x_{0,1} + x_{1,2}) \mathbb{1}_{\{x_{1,2} + \beta x_{0,1} \leq \lambda\}} + \frac{y_1}{y_0} (\lambda - x_{1,2} - \beta x_{0,1})^+ \\ &= -y_1 + (\beta x_{0,1} + x_{1,2}) \mathbb{1}_{\{x_{1,2} + \beta x_{0,1} \leq \lambda\}} + (\lambda - x_{1,2} - \beta x_{0,1})^+ \end{aligned}$$

and the statement follows immediately if $x_{1,2}(t) + \beta x_{0,1}(t) \leq \lambda$. On the other hand, if $x_{1,2}(t) + \beta x_{0,1}(t) > \lambda$, then, since $x_{0,2}(t) = 0$ and t is supposed to be a point of differentiability, we get (by (5c)) the contradiction that $0 = \dot{x}_{0,2}(t) = x_{1,2}(t) - h_0(x(t)) + \beta x_{0,1}(t) - \gamma x_{0,2}(t) = x_{1,2}(t) + \beta x_{0,1}(t) > \lambda$; the first equality holds because $x_{0,2}(t)$ is a non-negative absolutely continuous function. This shows that t cannot be a point of differentiability. Finally, if $y_0(t) = 0$, then the differentiability at t and the normalizing condition $\|x\| = 1$ give $0 = \dot{y}_0(t) = -\dot{x}_{0,0}(t) - \dot{x}_{0,1}(t) = \beta x_{0,1}$ and thus $x_{0,0}(t) = 1$. Assumption 2 requires that $g(x) > 0$ when $x_{0,0} = 1$, so (5a) implies that $\dot{x}_{0,0} < 0$. This contradicts that t is a point of differentiability because $x_{0,0}(t)$ is uniformly bounded by one and absolutely continuous. \square

We now prove Theorem 3 by showing that $\|x(t) - x^*\| \rightarrow 0$ in each of the following complete and mutually exclusive cases. For each case, we show that $x(t)$ follows a unique trajectory that stays in \mathcal{S}_1 .

Case i). Suppose that $x_{0,2}(t) = 0$ for all $t \geq 0$. This rules out the possibility that $x_{0,0}(t)$ stays on zero for all t large enough because (5a) and (5b), together with the normalizing condition $\|x\| = 1$, would imply that $y_1(t) \rightarrow 1$ as $t \rightarrow \infty$, and in this case Lemma 9 yields the contradiction that $\overline{Q}(x(t))$ is eventually negative. Thus, without loss of generality, let us assume that $x_{0,0}(0) > 0$. Then, using (5), $x(t)$ satisfies

$$\dot{x}_{0,0} = -\alpha g(x) \quad (63a)$$

$$\dot{x}_{0,1} = \alpha g(x) - \beta x_{0,1} \quad (63b)$$

$$\dot{x}_{0,2} = 0, \quad x_{1,2} + \beta x_{0,1} \leq \lambda. \quad (63c)$$

Note that $\lim_{t \rightarrow \infty} x_{0,0}(t)$ exists, say $x_{0,0}(\infty)$, because $\dot{x}_{0,0}(t) \leq 0$ and $x_{0,0}(t)$ is uniformly bounded. Thus, as $t \rightarrow \infty$, $\dot{x}_{0,0}(t) = -\alpha g(x(t)) \rightarrow 0$. Given the assumptions on g , $(\lambda - x_{0,1}(t) - \beta x_{1,2}(t))^+ \rightarrow 0$ and since $x_{1,2}(t) + \beta x_{0,1}(t) \leq \lambda$ for all t , by (63c), we obtain that $x_{1,2}(t) + \beta x_{0,1}(t) \rightarrow \lambda$. Then, (63b) and $g(x(t)) \rightarrow 0$ imply that $x_{0,1}(t) \rightarrow 0$ and thus $x_{1,2}(t) \rightarrow \lambda$. In turn, (5d) gives $x_{i,2}(t) \rightarrow 0$ for all $i \geq 2$, and the normalizing condition $\|x\| = 1$ implies that necessarily $x_{0,0}(t) \rightarrow 1 - \lambda$. Thus, $\|x(t) - x^*\| \rightarrow 0$.

Case ii). Suppose that $x_{0,2}(t) > 0$ for all t . Then, $x(t)$ satisfies the following conditions (using Definition 1)

$$\dot{x}_{0,0} = \gamma x_{0,2} - \alpha g \mathbb{I}_{\{x_{0,0} > 0\}} - \gamma x_{0,2} \mathbb{I}_{\{x_{0,0} = 0, \gamma x_{0,2} \leq \alpha g\}} \quad (64a)$$

$$\dot{x}_{0,1} = \alpha g \mathbb{I}_{\{x_{0,0} > 0\}} - \beta x_{0,1} + \gamma x_{0,2} \mathbb{I}_{\{x_{0,0} = 0, \gamma x_{0,2} \leq \alpha g\}} \quad (64b)$$

$$\dot{x}_{0,2} = x_{1,2} - \lambda + \beta x_{0,1} - \gamma x_{0,2} \quad (64c)$$

$$\dot{x}_{1,2} = x_{2,2} - x_{1,2} + \lambda \quad (64d)$$

$$\dot{x}_{i,2} = x_{i+1,2} \mathbb{I}_{\{i < B\}} - x_{i,2}, \quad i \geq 2. \quad (64e)$$

The ODE system (64d)-(64e) is an autonomous linear ODE system with constant coefficients and, developing the matrix-exponential general solution of such ODE system, for all $i \geq 1$ we obtain

$$x_{i,2}(t) = \lambda \mathbb{I}_{\{i=1\}} + e^{-t} \sum_{k=i}^B \frac{t^{k-i}}{(k-i)!} (x_{k,2}(0) - \lambda \mathbb{I}_{\{k=1\}}) \quad (65)$$

and thus $x_{i,2}(t) \rightarrow \lambda \mathbb{I}_{\{i=1\}}$ as $t \rightarrow \infty$. In turn, $\lim_{t \rightarrow \infty} (\lambda - x_{1,2}(t) - \beta x_{0,1}(t))^+ = \lim_{t \rightarrow \infty} (-\beta x_{0,1}(t))^+ = 0$ and therefore $g(x(t)) \rightarrow 0$. Since $g(x(t)) \rightarrow 0$, $x_{0,1}(t) \rightarrow 0$ necessarily by (64b), and using this in (64c) we obtain $x_{0,2}(t) \rightarrow 0$. Since $\|x\| = 1$, necessarily $x_{0,0}(t) \rightarrow 1 - \lambda$ and we have shown that $\|x(t) - x^*\| \rightarrow 0$.

Case iii). If the conditions in cases *i)* and *ii)* are not met, then there exists t_0, t_1 , with $t_0 \leq t_1 < \infty$, and $\delta > 0$ such that

1. $x_{0,2}(t) = 0$ for all $t \in [t_0, t_1]$
2. $x_{0,2}(t) > 0$ and $\dot{x}_{0,2}(t) < 0$ for all $t \in [t_0 - \delta, t_0)$, and
3. $x_{0,2}(t) > 0$ and $\dot{x}_{0,2}(t) > 0$ for all $t \in (t_1, t_1 + \delta]$.

On $[t_0 - \delta, t_0)$, $h_0(x(t)) = \lambda$ (by (7)) and using (5c), we obtain $\dot{x}_{0,2}(t) = x_{1,2}(t) - \lambda + \beta x_{0,1}(t) - \gamma x_{0,2}(t) < 0$ and thus by continuity

$$0 \geq \lim_{t \uparrow t_0} x_{1,2}(t) - \lambda + \beta x_{0,1}(t) - \gamma x_{0,2}(t) = x_{1,2}(t_0) - \lambda + \beta x_{0,1}(t_0). \quad (66)$$

Since $x_{0,2}(t_0) = 0$ on $[t_0, t_1]$, (5c) implies that (66) holds as well on $[t_0, t_1]$. On $(t_1, t_1 + \delta]$, $h_0(x(t)) = \lambda$ (by (7)) and using again (5c), we obtain

$$0 < \dot{x}_{0,2}(t) = x_{1,2}(t) - h_0(x(t)) + \beta x_{0,1}(t) - \gamma x_{0,2}(t) < x_{1,2}(t) - \lambda + \beta x_{0,1}(t) \quad (67)$$

and therefore $g(x(t)) = 0$. By continuity of fluid solutions, $x_{1,2}(t_1) + \beta x_{0,1}(t_1) = \lambda$. In addition, on $(t_1, t_1 + \delta]$, $x(t)$ is uniquely defined by

$$\dot{x}_{0,0} = \gamma x_{0,2} \quad (68a)$$

$$\dot{x}_{0,1} = -\beta x_{0,1} \quad (68b)$$

$$\dot{x}_{0,2} = x_{1,2} - \lambda + \beta x_{0,1} - \gamma x_{0,2} \quad (68c)$$

$$\dot{x}_{1,2} = x_{2,2} - x_{1,2} + \lambda \quad (68d)$$

$$\dot{x}_{i,2} = x_{i+1,2} \mathbb{1}_{\{i < B\}} - x_{i,2}, \quad i \geq 2, \quad (68e)$$

and we also know that $\dot{x}_{0,2}(t) > 0$. As long as *a)* $g(x(t)) = 0$ and *b)* $x_{0,2}(t) > 0$, on $[t_1, \infty)$ the fluid solution under investigation $x(t)$ is indeed uniquely given by the trajectory induced by (68) on $[t_1, \infty)$. In the remainder, we show that both *a)* and *b)* hold true for all t . This will conclude the proof because x^* is the unique fixed point of (68) and because (68) is a linear ODE system with constant coefficients. For simplicity of notation, let us shift time and assume that $t_1 = 0$. Now, since $x_{0,1}(t) = x_{0,1}(0)e^{-\beta t}$ (by (68b)) and since $x_{1,2}(t)$ takes the form given in (65), substituting in (68c) we obtain

$$\begin{aligned} \dot{x}_{0,2}(t) &= \beta x_{0,1}(0)e^{-\beta t} - \gamma x_{0,2}(t) + e^{-t}(x_{1,2}(0) - \lambda) + e^{-t} \sum_{k=2}^B \frac{t^{k-1}}{(k-1)!} x_{k,2}(0) \\ &= \beta x_{0,1}(0)e^{-\beta t} - \gamma x_{0,2}(t) - \beta x_{0,1}(0)e^{-t} + e^{-t} \sum_{k=2}^B \frac{t^{k-1}}{(k-1)!} x_{k,2}(0) \\ &\geq \beta x_{0,1}(0)(e^{-\beta t} - e^{-t}) - \gamma x_{0,2}(t). \end{aligned}$$

Thus, $x_{0,2}(t) \geq z(t)$ where $z(t)$ is uniquely defined by $\dot{z}(t) = \beta x_{0,1}(0)(e^{-\beta t} - e^{-t}) - \gamma z(t)$ with $z(0) = x_{0,2}(0)$. The solution of this differential equation is

$$z(t) = \beta x_{0,1}(0)e^{-\gamma t} \left(\frac{1 - e^{-t(\beta-\gamma)}}{\beta - \gamma} - \frac{1 - e^{-t(1-\gamma)}}{1 - \gamma} \right)$$

and now we notice that $z(t) > 0$ if $\beta > 1$, for all t . This proves property *b)*. To prove property *a)*, we use again (65) and $x_{1,2}(t_1) + \beta x_{0,1}(t_1) = \lambda$ to obtain

$$x_{1,2}(t) + \beta x_{0,1}(t) - \lambda = \beta x_{0,1}(0) (e^{-\beta t} - e^{-t}) + e^{-t} \sum_{k=2}^B \frac{t^{k-1}}{(k-1)!} x_{k,2}(0) > 0, \quad (69)$$

where the last inequality follows because $\beta < 1$. Given (17), (69) implies $g(x(t)) = 0$.

8 Proofs of Technical Lemmas

8.1 Proof of Lemma 4

We give a proof for the first limit because the argument used for the others is identical.

Since $t_n \in (t, t + \epsilon]$ whenever $n \in \{\mathcal{N}_\phi(N_k t) + 1, \dots, \mathcal{N}_\phi(N_k(t + \epsilon))\}$, (31) implies that for all k sufficiently large $|Y_i^{N_k}(t_n) - \sum_{j=0}^i \bar{x}_{j,2}(t)| \leq C\epsilon$, for some constant C , i.e.,

$$\mathbf{1}_{(\sum_{j=0}^i \bar{x}_{j,2}(t) + C\epsilon, \sum_{j=0}^i \bar{x}_{j,2}(t) - C\epsilon]} \leq \mathbf{1}_{(Y_i^{N_k}(t_n), Y_i^{N_k}(t_n))} \leq \mathbf{1}_{(\sum_{j=0}^i \bar{x}_{j,2}(t) - C\epsilon, \sum_{j=0}^i \bar{x}_{j,2}(t) + C\epsilon)} \quad (70)$$

Let Γ denote the LHS of the first equation in Lemma 4. Applying Lemma 1, we obtain

$$\Gamma \leq \lim_{\epsilon \downarrow 0} \lim_{k \rightarrow \infty} \frac{1}{\epsilon N_k} \sum_{n=\mathcal{N}_\phi(N_k t)+1}^{\mathcal{N}_\phi(N_k(t+\epsilon))} \mathbb{1}_{\{W_n=1\}} \mathbf{1}_{(\sum_{j=0}^i \bar{x}_{j,2}(t) - C\epsilon, \sum_{j=0}^i \bar{x}_{j,2}(t) + C\epsilon)} = \bar{x}_{i,2}(t)$$

and using (70) in the other direction we obtain $\Gamma = \bar{x}_{i,2}(t)$ as desired.

8.2 Proof of Lemma 6

We recall that we have analyzed \bar{x} along a fixed $\omega \in \mathcal{C}$, where $\mathbb{P}(\mathcal{C}) = 1$. We now explicit the dependence on ω and treat quantities $\bar{x}(t)$ and $X^N(t)$ as random variables. Let

$$Z_n^N := \mathbf{1}_{\substack{A_n^1(1-X_{0,0}^N(t_n^-)-X_{0,1}^{N,k}(t_n^-)) \\ (Y_{i-1}^N(t_n^-), Y_i^N(t_n^-))}} \mathbb{I}_{\{\sum_{j=0}^d X_{j,2}^N(t_n^-) > 0\}}. \quad (71)$$

For all n , the random variable Z_n^N is \mathcal{F}_n -measurable where $\mathcal{F}_n := \{X^N(t_n^{N,\lambda^-}), A_n^1, W_n\}$, and

$$\mathbb{E}[Z_n^N | \mathcal{F}_n \setminus A_n^1] = \frac{X_{i,2}^N(t_n^-)}{1 - X_{0,0}^N(t_n^-) - X_{0,1}^N(t_n^-)} \mathbb{I}_{\{\sum_{j=0}^d X_{j,2}^N(t_n^-) > 0\}} \quad (72)$$

where the set $\mathcal{F}_n \setminus W_n$ denotes the set \mathcal{F}_n with A_n^1 removed. Now, let $\Delta_n^N := Z_n^N - \mathbb{E}[Z_n^N | \mathcal{F}_n \setminus W_n]$. Then, $\mathbb{E}[\Delta_n^N | \mathcal{F}_n \setminus W_n] = 0$ and $|\Delta_n^N| \leq 2$, and applying the Azuma–Hoeffding inequality, we get

$$\mathbb{P}\left(\frac{1}{N} \left| \sum_{n=1}^N \Delta_n^N \right| > \delta\right) \leq 2 \exp\left(-\frac{(N\delta)^2}{8N}\right) \quad (73)$$

for any $\delta > 0$. Since $\sum_N \exp(-N\delta^2/8) < \infty$, an application of the Borel–Cantelli lemma shows that $\frac{1}{N} \sum_{n=1}^N \Delta_n^N \rightarrow 0$ almost surely. In particular,

$$\lim_{N \rightarrow \infty} \frac{1}{\epsilon N} \sum_{\substack{n=\mathcal{N}_\phi(Nt)+1: \\ W_n=0}}^{\mathcal{N}_\phi(N(t+\epsilon))} \mathbf{1}_{\substack{A_n^1(1-X_{0,0}^N(t_n^-)-X_{0,1}^{N,k}(t_n^-)) \\ (Y_{i-1}^N(t_n^-), Y_i^N(t_n^-))}} \left(\mathbb{I}_{\{\sum_{j=0}^d X_{j,2}^N(t_n^-) > 0\}} - \mathbb{E}[Z_n^N | \mathcal{F}_n \setminus W_n] \right) = 0 \quad (74)$$

almost surely. We now come back to work on a given trajectory ω . In view of the previous equality, we may redefine \mathcal{C} in Lemma 1 to be a subset of \mathcal{C}' where $\mathbb{P}(\mathcal{C}' = 1)$ and (74) holds for all $\omega \in \mathcal{C}'$. Therefore, we fix $\omega \in \mathcal{C}$ and use (31) and (72) to obtain that

$$\begin{aligned} \lim_{k \rightarrow \infty} \frac{1}{\epsilon N_k} \sum_{\substack{n=\mathcal{N}_\phi(N_k t)+1: \\ W_n=0}}^{\mathcal{N}_\phi(N_k(t+\epsilon))} \mathbb{E}[Z_n^{N_k} | \mathcal{F}_n \setminus W_n] \mathbb{I}_{\{\sum_{j=0}^d X_{j,2}^{N_k}(t_n^-) > 0\}} \\ \leq \lim_{k \rightarrow \infty} \frac{1}{\epsilon N_k} \sum_{\substack{n=\mathcal{N}_\phi(N_k t)+1: \\ W_n=0}}^{\mathcal{N}_\phi(N_k(t+\epsilon))} \frac{\bar{x}_{i,2}(t) + \delta}{1 - \bar{x}_{0,0}(t) - \bar{x}_{0,1}(t) - \delta} \mathbb{I}_{\{\sum_{j=0}^d X_{j,2}^{N_k}(t_n^-) > 0\}} \end{aligned}$$

for any $\delta > 0$ sufficiently small. Replacing δ by $-\delta$ in the last fraction term, the previous inequality can be reversed and letting $\delta \downarrow 0$, we obtain

$$\begin{aligned} \lim_{k \rightarrow \infty} \frac{1}{\epsilon N_k} \sum_{\substack{n=\mathcal{N}_\phi(N_k t)+1: \\ W_n=0}}^{\mathcal{N}_\phi(N_k(t+\epsilon))} \mathbb{E}[Z_n^{N_k} | \mathcal{F}_n \setminus W_n] \mathbb{I}_{\{\sum_{j=0}^d X_{j,2}^{N_k}(t_n^-) > 0\}} \\ = \frac{\bar{x}_{i,2}(t)}{1 - \bar{x}_{0,0}(t) - \bar{x}_{0,1}(t)} \lim_{k \rightarrow \infty} \frac{1}{\epsilon N_k} \sum_{\substack{n=\mathcal{N}_\phi(N_k t)+1: \\ W_n=0}}^{\mathcal{N}_\phi(N_k(t+\epsilon))} \mathbb{I}_{\{\sum_{j=0}^d X_{j,2}^{N_k}(t_n^-) > 0\}} \quad (75) \end{aligned}$$

Finally, (75) and (74) give (47).

8.3 Proof of Lemma 8

Let $w_d := \sum_{j=0}^d x_{j,2}$. For now, let us assume that $x_{0,2} > 0$. In this case, $w_d > 0$ and (57) boils down to (by (7))

$$x_{1,2} = \frac{\lambda}{w_d} x_{0,2} \quad (76a)$$

$$x_{i+1,2} = x_{i,2} + \frac{\lambda}{w_d}(x_{i,2} - x_{i-1,2}), \quad i = 1, \dots, d \quad (76b)$$

$$x_{d+2,2} = x_{d+1,2} - \frac{\lambda}{w_d}x_{d,2} \quad (76c)$$

$$x_{i+1,2} = x_{i,2}, \quad i \geq d+2. \quad (76d)$$

Since $\|x\| = 1$, (76) holds if and only if $x_{i,2} = 0$ for all $i \geq d+2$ and

$$x_{i,2} = \left(\frac{\lambda}{w_d}\right)^i x_{0,2}, \quad i = 0, \dots, d+1. \quad (77)$$

If $d = 0$, then $w_d = x_{0,2}$ and $x_{1,2} = \lambda$, and the lemma is proven. Thus, let $d \geq 1$. Summing (77) over $i = 0, \dots, d$, we obtain

$$w_d = \frac{1 - \left(\frac{\lambda}{w_d}\right)^{d+1}}{1 - \frac{\lambda}{w_d}} x_{0,2} \quad (78)$$

and letting $z_d := \sum_{j=1}^d x_{j,2}$ we obtain (9) as desired and it remains to prove (8a). Using (77), we notice that (9) holds if and only if

$$z_d + x_{0,2} = \frac{x_{0,2} - x_{d+1,2}}{1 - \frac{\lambda}{z_d + x_{0,2}}} \quad (79)$$

and rearranging terms we obtain $z_d + x_{0,2} - \lambda = x_{0,2} - x_{d+1,2}$. Then, (8a) follows by using the normalizing condition $\|x\| = 1$ as $x_i = 0$ for all $i \geq d+2$.

It remains to consider the case where $x_{0,2} = 0$. Here, $x_{0,2} = 0$ if and only if $x_{0,1} = 0$, by (56), which implies

$$g\mathbb{I}_{\{x_{0,0} > 0\}} = 0, \quad (80)$$

by (55b). In addition, if $w_d > 0$, then (57) boils down again to (76) and $x_{0,2} = 0$ would imply that $x_{i,2} = 0$ for all i . This is not possible in view of $\|x\| = 1$ and, therefore, we must have $w_d = 0$. Since necessarily $x_{0,0} < 1$, (7) simplifies to

$$h_i(x) = \begin{cases} x_{d+1,2}\mathbb{I}_{\{i=d\}}\mathbb{I}_{\{x_{d+1,2} \leq \lambda\}} & \text{if } i \leq d, \\ \frac{x_{i,2}}{1-x_{0,0}}(\lambda - x_{d+1,2})^+ & \text{if } i > d \end{cases} \quad (81)$$

and substituting in (58) we get

$$x_{i,2} = 0, \quad i \leq d \quad (82a)$$

$$x_{d+1,2} = x_{d+1,2}\mathbb{I}_{\{x_{d+1,2} \leq \lambda\}} \quad (82b)$$

$$x_{i,2} = \frac{x_{i-1,2}}{1-x_{0,0}}(\lambda - x_{d+1,2})^+, \quad i \geq d+2. \quad (82c)$$

This gives (8f). Now, if $x_{d+1,2} > \lambda$, then (82b) is violated, and if $x_{d+1,2} = 0$, then (82c) and $\|x\| = 1$ give the contradiction that $1 = \lambda$. So, necessarily $x_{d+1,2} \in (0, \lambda]$, i.e., (8h). Here, we notice that $x_{d+1,2}$ is not tied to a specific value. Then, summing (82c) we obtain

$$\sum_{i \geq d+2} x_{i,2} = \sum_{i \geq d+2} \frac{x_{i-1,2}}{1-x_{0,0}}(\lambda - x_{d+1,2}), \quad (83)$$

which, using $\|x\| = 1$ and (82), holds if and only if

$$1 - x_{d+1,2} - x_{0,0} = \frac{\lambda - x_{d+1,2}}{1 - x_{0,0}}(1 - x_{0,0}) \quad (84)$$

i.e., if and only if $x_{0,0} = 1 - \lambda$; note that $x_{0,0} = 0$ is not possible as otherwise (82c) and $\|x\| = 1$ give the contradiction that $1 < \lambda$. Since $x_{0,0} > 0$, necessarily $g = 0$ by (80), which gives (8i). Using $x_{d+1,2} \leq \lambda$ and $x_{0,0} = 1 - \lambda$ in (82c), we obtain $x_{d+2,2} = x_{d+1,2}(1 - x_{d+1,2}/\lambda)$ and applying inductively (82c), we obtain (8g). This concludes the proof.

9 Proof of Proposition 1

The fact that x^* is a fixed point is trivial. Suppose that there exists $\delta > 0$ such that $x_{0,2}(t) > 0$ on $(0, \delta]$. Then, there exists $\delta' > 0$ such that $\dot{x}_{0,2}(t) > 0$ on $(0, \delta']$. Using (5c), which gives $\dot{x}_{0,2} = x_{1,2} - \lambda + \beta x_{0,1} - \gamma x_{0,2}$, we obtain

$$x_{1,2}(t) + \beta x_{0,1}(t) > \lambda + \gamma x_{0,2}(t), \quad \forall t \in (0, \delta'] \quad (85)$$

and thus $x_{1,2}(0) + \beta x_{0,1}(0) = \lim_{t \downarrow 0} x_{1,2}(t) + \beta x_{0,1}(t) \geq \lambda$, by continuity of the fluid model. This contradicts the last condition in (14) and thus $x_{0,2}(t) = 0$ on a right neighborhood of zero, say $[0, \delta]$. Since $g(x) = \lambda - 1 + x_{0,0}$, on $[0, \delta]$ we obtain (using (5))

$$\dot{x}_{0,0} = -\alpha(\lambda - 1 + x_{0,0}) \quad (86a)$$

$$\dot{x}_{0,1} = \alpha(\lambda - 1 + x_{0,0}) - \beta x_{0,1} \quad (86b)$$

$$\dot{x}_{0,2} = 0 \quad (86c)$$

$$\dot{x}_{i,2} = x_{i+1,2} - x_{i,2} + h_{i-1}(x) - h_i(x), \quad i \geq 1 \quad (86d)$$

where

$$h_i(x) = \begin{cases} \beta x_{0,1} + x_{1,2} & \text{if } i = 0, \\ \frac{x_{i,2}}{y_1}(\lambda - x_{1,2} - \beta x_{0,1})^+ & \text{if } i > 0. \end{cases} \quad (87)$$

We observe that (86a)-(86b) form an autonomous linear ODE system. By continuity of $x(t)$, (14) holds as well on a right neighborhood of zero. Now, we actually show that (14) holds on $[0, \infty)$, i.e., $\delta = +\infty$. Towards this purpose, let us analyze the system (86a)-(86b) in isolation. After some algebra, we obtain

$$x_{0,0}(t) = 1 - \lambda + (x_{0,0} - 1 + \lambda)e^{-\alpha t} \quad (88a)$$

$$x_{0,1}(t) = \frac{\alpha(x_{0,0} - 1 + \lambda)}{\beta - \alpha}(e^{-\alpha t} - e^{-\beta t}) + x_{0,1}(0)e^{-\beta t}. \quad (88b)$$

Thus,

- i) $x_{0,0}(t)$ monotonically decreases to zero as $t \rightarrow \infty$, and
- ii) $y_0(t) = y_1(t) < 1$ with both $y_0(t)$ and $y_1(t)$ monotonically increasing to λ because $\dot{x}_{0,0} + \dot{x}_{0,1}$ is always non-increasing and $x_{0,2}$ stays on zero.

To prove that (14) holds on $[0, \infty)$, it remains to show that $x_{1,2}(t) + \beta x_{0,1}(t) < \lambda$ for all $t \geq 0$. This property is true because $x_{1,2} + \beta x_{0,1} \leq y_1 + x_{0,1} = 1 - x_{0,0} = \lambda - (x_{0,0}(0) - 1 + \lambda)e^{-\alpha t} < \lambda$. Thus, $x(t)$ satisfies (86) on $[0, \infty)$. In addition, since $x_{0,0}(0) + x_{0,1}(0) < 1$ and $\dot{x}_{0,0}(t) + \dot{x}_{0,1}(t) = -\beta x_{0,1}(t) \leq 0$ for all t , the drift function of (86) is Lipschitz and therefore it induces a unique flow [14, page 56]. Since $x_{0,0}(t) \downarrow 1 - \lambda$ as $t \rightarrow \infty$, for all $t \geq 0$

$$\dot{\bar{Q}}(x(t)) = \lambda - y_1(t) = x_{0,0}(t) + x_{0,1}(t) + \lambda - 1 \geq x_{0,0}(t) + \lambda - 1 > 0, \quad (89)$$

where the first equality follows by Lemma 9. In particular, $\lim_{t \rightarrow \infty} \bar{Q}(x(t))$ exists and must be greater than λ because $\lambda < \bar{Q}(x(0)) < \infty$. Combining (88) and (89), we obtain

$$\begin{aligned} \dot{\bar{Q}}(x(t)) &= (x_{0,0}(0) - 1 + \lambda)e^{-\alpha t} + \frac{\alpha(x_{0,0}(0) - 1 + \lambda)}{\beta - \alpha}(e^{-\alpha t} - e^{-\beta t}) + x_{0,1}(0)e^{-\beta t} \\ &= \underbrace{\frac{\beta(x_{0,0}(0) - 1 + \lambda)}{\beta - \alpha}}_{:=C_1} e^{-\alpha t} + \underbrace{\left(x_{0,1}(0) - \frac{\alpha(x_{0,0}(0) - 1 + \lambda)}{\beta - \alpha} \right)}_{:=C_2} e^{-\beta t}. \end{aligned}$$

Integrating,

$$\bar{Q}(x(t)) = \bar{Q}(x(0)) + \frac{C_1}{\alpha}(1 - e^{-\alpha t}) + \frac{C_2}{\beta}(1 - e^{-\beta t})$$

$$\xrightarrow{t \rightarrow \infty} \bar{Q}(x(0)) + \frac{\alpha + \beta}{\alpha\beta}(x_{0,0}(0) - 1 + \lambda) + \frac{1}{\beta}x_{0,1}(0)$$

which proves (16). Finally, suppose that $\lim_{t \rightarrow \infty} x_{1,2}(t)$ exists, say $x_{1,2}(\infty)$. Then, necessarily $x_{1,2}(\infty) < \lambda$ because $y_1(t) \rightarrow \lambda$ and $\lim_{t \rightarrow \infty} Q(x(t)) > \lambda$ excludes that $x_{1,2}(t) \rightarrow \lambda$. Then, using (86d) when $i = 1$ and that $x_{1,2}(t)$ is Lipschitz continuous,

$$\begin{aligned} 0 &= \lim_{t \rightarrow \infty} \dot{x}_{1,2}(t) = \lim_{t \rightarrow \infty} x_{2,2} + \beta x_{0,1} - \frac{x_{1,2}}{1 - x_{0,0} - x_{0,1}}(\lambda - x_{1,2} - \beta x_{0,1}) \\ &= \lim_{t \rightarrow \infty} \left(x_{2,2} - \frac{x_{1,2}}{\lambda}(\lambda - x_{1,2}) \right) = -x_{1,2}(\infty) \left(1 - \frac{x_{1,2}(\infty)}{\lambda} \right) + \lim_{t \rightarrow \infty} x_{2,2}, \end{aligned}$$

which shows that $\lim_{t \rightarrow \infty} x_{2,2}$ must exist as well and be equal to $x_{1,2}(\infty) \left(1 - \frac{x_{1,2}(\infty)}{\lambda} \right)$. By induction, $\lim_{t \rightarrow \infty} x_{i,2}$ exists and is equal to $x_{i,2}(\infty) \left(1 - \frac{x_{1,2}(\infty)}{\lambda} \right)^{i-1}$. Thus, $x(\infty) \in \mathcal{S}_{\text{subopt}}$.